Human Molecular Genetics, 2014, Vol. 23, No. 19 **5171–5187**
doi:10.1093/hmg/ddu240
Advance Access published on May 15, 2014

Haplotype-specific modulation of a SOX10/CREB response element at the Charcot–Marie–Tooth disease type 4C locus *SH3TC2*

Megan Hwa Brewer[1], Ki Hwan Ma[4], Gary W. Beecham[7], Chetna Gopinath[3], the Inherited Neuropathy Consortium (INC), Frank Baas[8], Byung-Ok Choi[9], Mary M. Reilly[10], Michael E. Shy[11,12,13], Stephan Züchner[7], John Svaren[5,6] and Anthony Antonellis[1,2,3,*]

[1]Department of Human Genetics, [2]Department of Neurology and [3]Cellular and Molecular Biology Program, University of Michigan Medical School, Ann Arbor, MI, USA, [4]Cellular and Molecular Pathology (CMP) Program, [5]Waisman Center and [6]Department of Comparative Biosciences, University of Wisconsin-Madison, Madison, WI, USA, [7]Dr John T. Macdonald Foundation Department of Human Genetics and John P. Hussman Institute for Human Genomics, University of Miami Miller School of Medicine, Miami, FL, USA, [8]Department of Genome Analysis, Academic Medical Centre, Amsterdam, The Netherlands, [9]Department of Neurology, Samsung Medical Center, Sungkyunkwan University School of Medicine, Gangnam-Gu, Seoul, Korea, [10]MRC Centre for Neuromuscular Diseases, UCL Institute of Neurology, Queen Square, London, UK, [11]Department of Neurology, [12]Department of Pediatrics and [13]Department of Physiology, Carver College of Medicine, University of Iowa, Iowa City, IA, USA

Received March 12, 2014; Revised May 1, 2014; Accepted May 12, 2014

Loss-of-function mutations in the Src homology 3 (SH3) domain and tetratricopeptide repeats 2 (*SH3TC2*) gene cause autosomal recessive demyelinating Charcot–Marie–Tooth neuropathy. The SH3TC2 protein has been implicated in promyelination signaling through axonal neuregulin-1 and the ERBB2 Schwann cell receptor. However, little is known about the transcriptional regulation of the *SH3TC2* gene. We performed computational and functional analyses that revealed two *cis*-acting regulatory elements at *SH3TC2*—one at the promoter and one ~150 kb downstream of the transcription start site. Both elements direct reporter gene expression in Schwann cells and are responsive to the transcription factor SOX10, which is essential for peripheral nervous system myelination. The downstream enhancer harbors a single-nucleotide polymorphism (SNP) that causes an ~80% reduction in enhancer activity. The SNP resides directly within a predicted binding site for the transcription factor cAMP response element binding protein (CREB), and we demonstrate that this regulatory element binds to CREB and is activated by CREB expression. Finally, forskolin induces *Sh3tc2* expression in rat primary Schwann cells, indicating that *SH3TC2* is a CREB target gene. These findings prompted us to determine if SNP genotypes at *SH3TC2* are associated with differential phenotypes in the most common demyelinating peripheral neuropathy, CMT1A. Interestingly, this revealed several associations between SNP alleles and disease severity. In summary, our data indicate that *SH3TC2* is regulated by the transcription factors CREB and SOX10, define a regulatory SNP at this disease-associated locus and reveal *SH3TC2* as a candidate modifier locus of CMT disease phenotypes.

INTRODUCTION

Charcot–Marie–Tooth (CMT) disease is a clinically and genetically heterogeneous group of inherited peripheral neuropathies that affect motor and sensory neurons. Clinical presentations include muscle wasting, foot deformities and impaired sensation (1). Mutations in the Src homology 3 (SH3) domain and tetratricopeptide

*To whom correspondence should be addressed at: University of Michigan Medical School, 3710A Medical Sciences II, 1241 E. Catherine Street, Ann Arbor, MI 48109, USA. Tel: +1 7346474058; FAX: +1 7347633784; Email: antonell@umich.edu

repeats 2 (*SH3TC2*) gene cause autosomal recessive CMT type 4C (CMT4C) (2). CMT4C is the most common form of autosomal recessive demyelinating CMT disease, accounting for up to 26% of all cases (2–5). As with other subtypes of CMT disease, patients with CMT4C show variability of disease onset and severity (2,4). For example, onset of disease can vary from 2 to 50 years of age and the motor phenotype varies from mild gait disabilities to impairment requiring canes or wheelchairs. Furthermore, ∼60% of patients with CMT4C have scoliosis (2–4). Thus, there are likely genetic and environmental factors that modify the CMT4C phenotype.

SH3TC2 is expressed specifically in Schwann cells (6) and encodes a protein with SH3 and tetratricopeptide domains important for protein–protein interactions. SH3TC2 localizes to the endocytic recycling pathway (6–9) and interacts with the GTPase Rab11, a known regulator of recycling endosomes. Interestingly, mutant forms of SH3TC2 are unable to associate with Rab11 *in vitro,* suggesting that disease-associated *SH3TC2* mutations affect the rate of endosome recycling (8,9). It was recently shown that SH3TC2 plays a role in neuregulin-1 (Nrg1)/ERBB signaling, which is critical for the proliferation and migration of Schwann cells and the subsequent myelination of peripheral nerve axons (10). Specifically, SH3TC2 interacts with and internalizes ERBB2 and depletion of SH3TC2 *in vivo* results in downregulation of key ERBB targets (11). Indeed, two CMT4C-associated missense mutations that map to the interaction domain prevent internalization of ERBB2.

Over 30 *SH3TC2* mutations have been identified in patients with CMT4C in either a homozygous or compound heterozygous state. The majority of the mutations act via a loss-of-function mechanism and disease-associated alleles include nonsense, missense and splice-site mutations (2,3,12–16). Despite the loss-of-function nature of known pathogenic variants, regulatory mutations (e.g. those in promoters or enhancers) have not been identified at *SH3TC2*. Interestingly, the identification of patients with a CMT4C phenotype that are heterozygous for a single *SH3TC2* coding mutation (15,16) suggests that mutations at a second locus or mutations in non-coding, transcriptional regulatory elements at *SH3TC2* account for a certain portion of CMT4C disease.

Currently, little is known about the transcriptional regulation of *SH3TC2*. Addressing this issue will be important for fully understanding the biology of the *SH3TC2* locus and for identifying the full spectrum of disease-associated *SH3TC2* mutations. This information will also assist the identification of functional polymorphisms or modifiers that, by altering *SH3TC2* gene expression, may contribute to the variable clinical phenotype observed in patients with CMT4C or other CMT subtypes with a myelin-based pathology, such as the most common form of CMT disease: CMT1A caused by duplication of the peripheral myelin protein 22 *(PMP22)* (17–19). Here, we employ computational and functional analyses to identify transcriptional regulatory elements at *SH3TC2* and report the characterization of the *SH3TC2* promoter and a downstream enhancer. Interestingly, the latter element harbors a common single-nucleotide polymorphism (SNP) that dramatically decreases regulatory function. These findings provide key information regarding the biology of the *SH3TC2* locus and reveal candidate sequences for mutations and modifiers of CMT disease.

RESULTS

SH3TC2 harbors seven putative transcriptional regulatory elements

Multiple-species comparative sequence analysis is a powerful tool for predicting *cis*-acting transcriptional regulatory elements (20). To identify evolutionarily conserved sequences at *SH3TC2*, we aligned genomic sequences spanning *SH3TC2* and extending to the flanking loci (*ADRB2* and *ABLIM3*) from human, mouse, rat, dog, cow and opossum using MultiPipMaker software (21). Next, we identified non-coding, non-repetitive genomic sequences within the alignment that are at least 5 bp long and identical among all six species using ExactPlus (EP) (22). This analysis revealed 49 genomic segments ranging from 5 to 19 bp in length. Importantly, these smaller fragments fell into seven clusters of multiple-species conserved sequences (MCSs)—one directly upstream of the predicted transcription start site (TSS) of *SH3TC2*, one within the 3′ untranslated region and five downstream of *SH3TC2* (Table 1 and Fig. 1A). We considered these seven genomic segments to be candidate transcriptional regulatory elements for *SH3TC2*.

The *SH3TC2* promoter and *SH3TC2*-MCS5 direct luciferase expression in cultured Schwann cells

Our computational analyses revealed seven conserved genomic regions at the *SH3TC2* locus that potentially harbor transcriptional regulatory elements. To determine if these genomic segments have regulatory activity in relevant cells *in vitro*, we tested the ability of each to direct luciferase reporter gene expression in cultured Schwann (S16) cells. S16 cells are an immortalized rat Schwann cell line that exhibit a high transfection efficiency and express many myelin-related genes (e.g. *PMP22*, *MPZ*, *MBP* and *MAG*) and Schwann cell transcription factors (e.g. SOX10 and EGR2). Indeed, in a comparative analysis of gene expression in multiple Schwann cell lines, S16 cells were the most similar to myelinating Schwann cells (23). Briefly, each genomic segment (Table 1) was cloned upstream of a minimal promoter directing the expression of a luciferase reporter gene and each resulting construct was transfected into S16 cells. Luciferase activity was then measured compared with a control vector with no genomic insert ('Empty' in figures). To identify the most promising regulatory elements at *SH3TC2*, a 10-fold or higher increase in luciferase activity was considered indicative of 'strong' enhancer activity. *SH3TC2*-MCS1, MCS2, MCS3, MCS4 and MCS6 did not display 'strong' enhancer activity in Schwann cells (<5-fold each; Fig. 1B); however, *SH3TC2*-MCS1 (*P*-value 0.003) and *SH3TC2*-MCS4

Table 1. Multiple-species conserved sequences (MCSs) at SH3TC2

Element ID	Genomic location[a]	Size (bp)
SH3TC2-Promoter	chr5:148 422 779–148 423 445	667
SH3TC2-MCS1	chr5:148 188 297–148 188 683	387
SH3TC2-MCS2	chr5:148 189 329–148 189 715	387
SH3TC2-MCS3	chr5:148 192 623–148 193 023	401
SH3TC2-MCS4	chr5:148 203 383–148 203 846	464
SH3TC2-MCS5	chr5:148 272 774–148 273 158	385
SH3TC2-MCS6	chr5:148 346 393–148 346 955	563

[a]Coordinates are from the March 2006 UCSC Human Genome Browser (hg18).

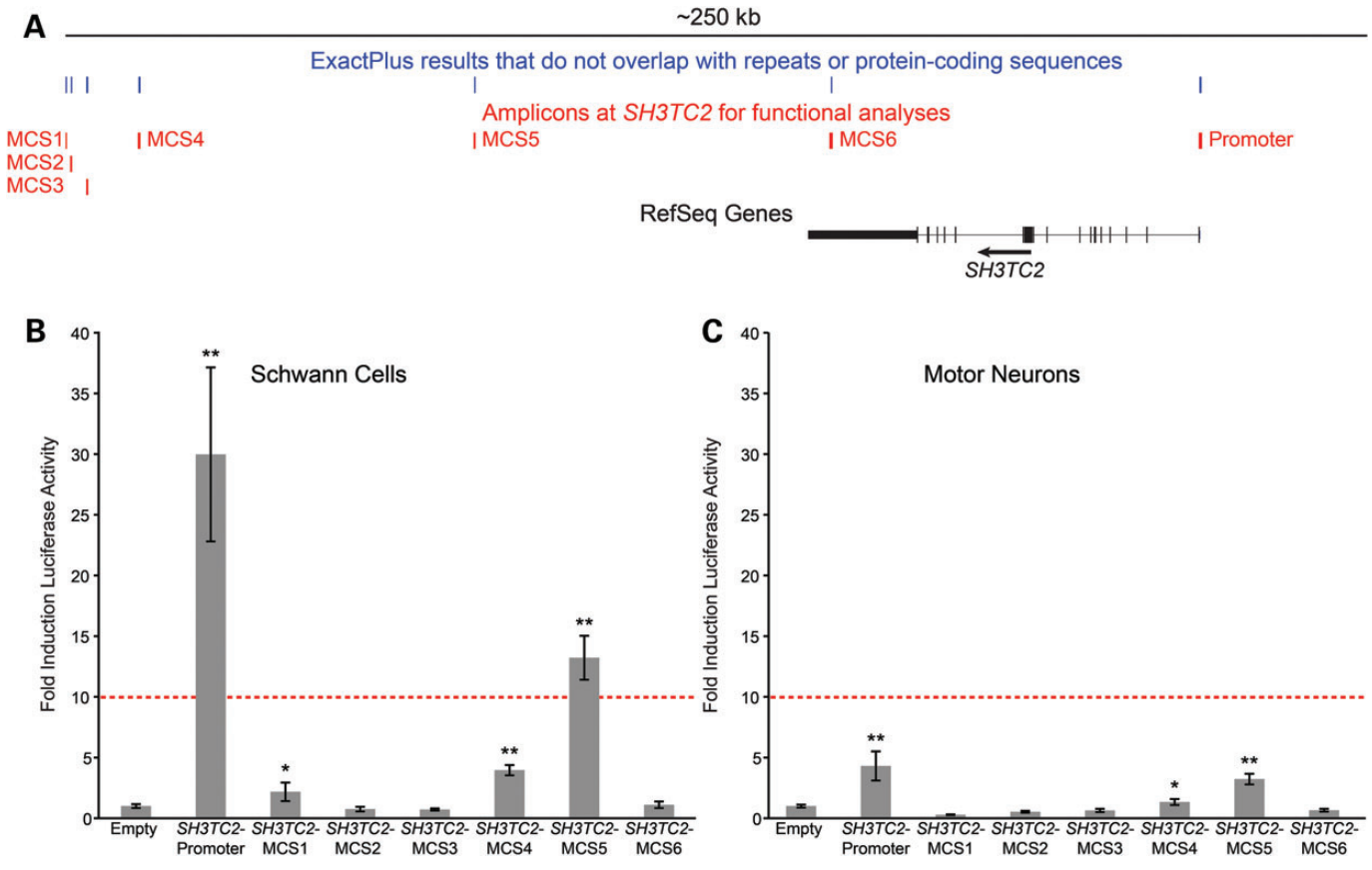

Figure 1. Identification of *cis*-acting transcriptional regulatory elements at *SH3TC2*. (**A**) The human *SH3TC2* locus is shown with transcription proceeding from right to left. Genomic segments at least 5 bp in length, conserved among six mammalian species, and that map outside of protein-coding and repetitive sequences [identified by ExactPlus (EP)] are indicated in blue. Clusters of EP hits that represent multiple-species conserved sequences (MCSs) and that were used to design PCR products for functional studies are indicated in red. (**B** and **C**) The promoter and each MCS were cloned upstream of a luciferase reporter gene and tested for regulatory activity in cultured Schwann (S16) cells (B) and motor neurons (MN-1 cells; C). All data are expressed relative to a control vector that does not harbor an insert ('Empty' in B and C), dashed red lines indicate the 10-fold cutoff for 'strong enhancer activity', error bars show standard deviations, and * and ** indicate a significant change in activity ($P \leq 0.01$ and $P \leq 0.001$, respectively).

(P-value 2.2×10^{-8}) did significantly increase reporter gene expression to a lesser degree (2.1- and 3.9-fold, respectively). In contrast, the *SH3TC2* promoter and *SH3TC2*-MCS5 demonstrated a 30-fold (P-value 8.74×10^{-6}) and 13-fold (P-value 2.34×10^{-7}) increase in activity, respectively, in these cells (Fig. 1B). To determine if the enhancer activities of the *SH3TC2* promoter and *SH3TC2*-MCS5 are specific to Schwann cells, each genomic segment at *SH3TC2* was reevaluated in a non-glial cell line—immortalized mouse motor (MN-1) neurons. Importantly, transcription factors important for Schwann cell function (e.g. SOX10) are not expressed in MN-1 cells (24). None of the regions tested displayed 'strong' enhancer activity in MN-1 cells. Indeed, the mean fold-induction of each of the seven tested genomic segments was <5 (Fig. 1C). Combined, these data suggest that the *SH3TC2* promoter and *SH3TC2*-MCS5 are important for transcriptional regulation of *SH3TC2* in Schwann cells.

The *SH3TC2* promoter harbors consensus sequences for Schwann cell transcription factors

The *SH3TC2* promoter studied here encompasses 667 bp upstream of the initiation codon (Fig. 2A). To characterize the position of the *SH3TC2* TSS in Schwann cells, we performed 5′ rapid amplification of cDNA ends (5′RACE). Briefly, *Sh3tc2* cDNA was generated from RNA isolated from cultured rat Schwann (S16) cells and 5′RACE was performed using a reverse primer in exon 4 of the rat *Sh3tc2* locus. The resulting PCR product was sequenced and aligned to rat genomic DNA sequences. These studies revealed a single *Sh3tc2* TSS located 37 bp upstream of the start codon in rat Schwann cells (Fig. 2A–C). This position also corresponds to 37 bp upstream of the initiating methionine codon at the human *SH3TC2* locus and differs from the current annotation of the *SH3TC2* RefSeq mRNA on the University of California at Santa Cruz (UCSC) Human Genome Browser (Fig. 2A).

SH3TC2 is specifically expressed in Schwann cells (6), suggesting that the locus is regulated by transcription factors important for these cells. To address this, we employed the TRANSFAC prediction algorithm (25) to search the *SH3TC2* promoter for the consensus sequences of three transcription factors critical for Schwann cells: SOX10, EGR2 and POU3F2 (26). These analyses revealed six SOX10 consensus sequences (bold text in Fig. 2C), one POU3F2 consensus sequence (red text in Fig. 2C) and one EGR2 consensus sequence (blue text

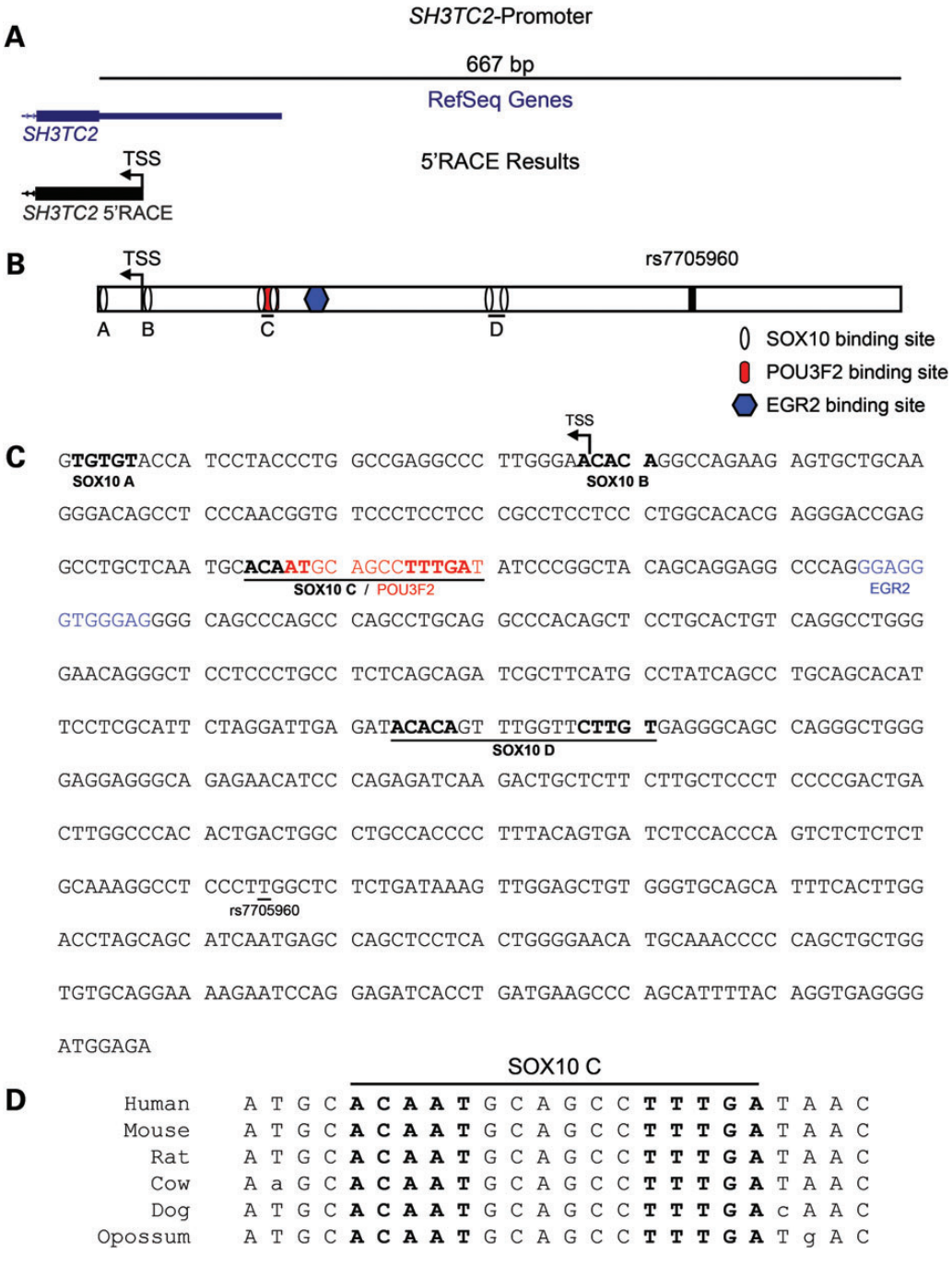

Figure 2. The *SH3TC2* promoter harbors multiple transcription factor consensus sequences relevant for Schwann cells. (**A**) The *SH3TC2* promoter (black line) spans 667 bp upstream of the initiating methionine codon based on the *SH3TC2* RefSeq mRNA (indicated in blue). 5′RACE was employed to identify the TSS of *SH3TC2* in cultured Schwann cells (indicated by the left-pointing black arrow). (**B**) Cartoon depicting the relative location of TRANSFAC binding site predictions in the *SH3TC2* promoter. The TSS identified in Schwann cells is indicated by the left-pointing arrow. Specific transcription factor binding predictions are indicated in the key and head-to-head SOX10 consensus sequences are underlined. The position of the SNP rs7705960 is indicated by a vertical black line. (**C**) Sequence of the *SH3TC2* promoter annotated with TRANSFAC binding site predictions. SOX10 (bold text), POU3F2 (red text) and EGR2 (blue text) predictions are indicated. Dimeric SOX10 head-to-head binding sites are underlined, as is the position of the rs7705960 SNP. (**D**) Orthologous sequences from the indicated species at the dimeric, head-to-head 'SOX10 C' consensus sequences were aligned. Individual SOX10 consensus sequences are in bold text and base pairs conserved between human and other species are capitalized.

in Fig. 2C). Note that the POU3F2 consensus sequence overlaps with one of the SOX10 consensus sequences. SOX10 is known to function as either a monomer or a dimer (22,27). As a monomer, SOX10 binds to a single SOX10 consensus sequence and as a dimer it binds to two consensus sequences oriented in a head-to-head fashion. Two of the SOX10 consensus sequences are consistent with binding to monomeric SOX10 (SOX10 A and SOX10 B in Fig. 2C) and four of the SOX10 consensus

sequences cluster into two head-to-head sequences consistent with binding to dimeric SOX10 (SOX10 C and SOX10 D in Fig. 2C). Note that the 'TTTGA' monomer (bold, red text in Fig. 2C) in the SOX10 C dimeric consensus sequence was not initially detected by our computational analyses (see Materials and Methods for details). However, we considered SOX10 C a potential head-to-head binding site due to the preferential 6 bp spacing (27) of the two monomeric predictions (Fig. 2C and D) and the conservation of the entire prediction among diverse mammalian species (Fig. 2D). Interestingly, reducing SOX10 function decreases the expression of *Sh3tc2* in Schwann cells (28,29) and SOX10 binding was previously detected at the *SH3TC2* promoter region by ChIP-Seq analysis of nuclei isolated from rat sciatic nerves (28) (also shown in Supplementary Material, Fig. S1A). The ChIP-Seq data directly overlap the SOX10 consensus sequences described above; however, the precise sequences responsible for SOX10 binding have not been identified.

SOX10 consensus sequences are necessary for the activity of the *SH3TC2* promoter

The presence of conserved SOX10 consensus sequences within the *SH3TC2* promoter suggests that these nucleotides are necessary for the observed regulatory activity in Schwann cells (Fig. 1B). To test this, we deleted or mutated each consensus sequence and tested the ability of the resulting genomic segment to direct luciferase reporter gene expression in cultured S16 cells compared with the wild-type *SH3TC2* promoter. For deletion analysis, the entire consensus sequence was removed from the construct ('Δ' in Fig. 3). For mutation analysis, the consensus sequence was mutagenized to complement but not reverse the sequence ('Mut' in Fig. 3). This should ablate the binding capabilities of the transcription factor while retaining the overall GC content of the genomic segment. Because SOX10 A and SOX10 B are palindromic (Fig. 2C) binding to SOX10 may not be disrupted by mutagenesis—we therefore only deleted these consensus sequences. Finally, deletion of the POU3F2 consensus sequence would also delete SOX10 C—we therefore mutated the 'GCAGCC' nucleotides between the two SOX10 consensus sequences in SOX10 C to only disrupt POU3F2 binding (Fig. 2C). Deletion of the SOX10 A and SOX10 B consensus sequences and mutagenesis of the POU3F2, EGR2 and SOX10 D consensus sequences did not significantly reduce the activity of the *SH3TC2* promoter (Fig. 3A). In contrast, mutagenesis and deletion of the SOX10 C consensus sequence resulted in an ∼60% (*P*-value 1.67×10^{-7}) and ∼50% (*P*-value 8.11×10^{-7}) reduction in enhancer activity, respectively, compared with the wild-type *SH3TC2* promoter (Fig. 3A). These data indicate that this SOX10 consensus sequence is required for the observed activity of the *SH3TC2* promoter.

Visual examination of the *SH3TC2* promoter at the UCSC Human Genome Browser revealed the presence of an SNP (rs7705960) with a minor allele frequency of 0.442 in individuals of European descent from the HapMap dataset. Since SNPs within transcriptional regulatory elements can affect gene transcription rates, we compared the enhancer activities of the major and minor alleles of rs7705960 in cultured Schwann cells in the context of the *SH3TC2* promoter (Table 1). These efforts revealed that the enhancer activity of the minor-allele harboring genomic segment (Fig. 3A) was similar to the segment carrying the major allele ('*SH3TC2*-Promoter' in Fig. 3A), indicating that this SNP does not affect the activity of the *SH3TC2* promoter.

SOX10 induces the activity of the *SH3TC2* promoter

Disrupting the head-to-head SOX10 C binding site causes a reduction in *SH3TC2* promoter activity, suggesting that SOX10 acts upon this element in Schwann cells. To determine if SOX10 induces the activity of the *SH3TC2* promoter we employed a SOX10 overexpression assay in SOX10-negative MN-1 cells. Briefly, a construct harboring the *SH3TC2* promoter upstream of a luciferase reporter gene was transfected into MN-1 cells with or without a construct harboring a CMV promoter directing wild-type SOX10 expression. In the presence of wild-type SOX10, the activity of the *SH3TC2* promoter dramatically increased (∼28-fold, *P*-value 7.36×10^{-10}; Fig. 3B).

If SOX10 is required for inducing *SH3TC2* promoter activity, then suppressing endogenous SOX10 activity in Schwann cells should cause a decrease in *SH3TC2* promoter activity. Certain mutations in the human *SOX10* gene (in the heterozygous state) result in a dominant-negative effect by disrupting the function of the wild-type SOX10 protein (30). We analyzed the activity of the *SH3TC2* promoter in the context of overexpressed, dominant-negative (E189X) SOX10 in S16 Schwann cells. Expression of dominant-negative SOX10 reduced the activity of the *SH3TC2* promoter by ∼73% (*P*-value 1.06×10^{-5}; Fig. 3C). Importantly, these data are consistent with studies showing that impairing SOX10 function reduces the expression of *Sh3tc2* in rat Schwann cell models (28,29). Combined, our studies indicate that SOX10 regulates the *SH3TC2* promoter via the SOX10 C binding site.

The minor allele of rs17539452 reduces *SH3TC2*-MCS5 activity in Schwann cells

Polymorphisms in *cis*-acting transcriptional regulatory elements can impact gene transcription and may be relevant for clinical phenotype variability. Examination of *SH3TC2*-MCS5 on the UCSC Human Genome Browser revealed that this genomic segment harbors six SNPs with a minor allele frequency of ≥0.01 (Fig. 4A). To determine if these SNPs alter the activity of *SH3TC2*-MCS5 in Schwann cells, we obtained four *SH3TC2*-MCS5 haplotypes via PCR amplification of pooled human DNA samples (Hap 1–4 in Fig. 4B). Hap 1 contains the major alleles of all six SNPs and represents the genomic segment tested in the initial luciferase assays (Fig. 1B). Hap 2 carries the minor alleles of two SNPs (rs12519780 and rs10875641) and corresponds to the reference sequence in the UCSC Human Genome Browser (hg19). Hap 3 carries the minor allele of rs12519780, and Hap 4 carriers the minor alleles of three SNPs: rs12519780, rs114059937 and rs17539452. Each haplotype was tested for the ability to direct luciferase reporter gene expression in S16 cells relative to Hap 1. The activity of *SH3TC2*-MCS5 Hap 2 and Hap 3 was not significantly decreased compared with Hap 1 (Fig. 4C). In contrast, the activities of Hap 4 was decreased by ∼80% (*P*-value 1.13×10^{-8}; Fig. 4C), and a decrease in activity were observed in both the forward and reverse orientation of the enhancer (Supplementary Material,

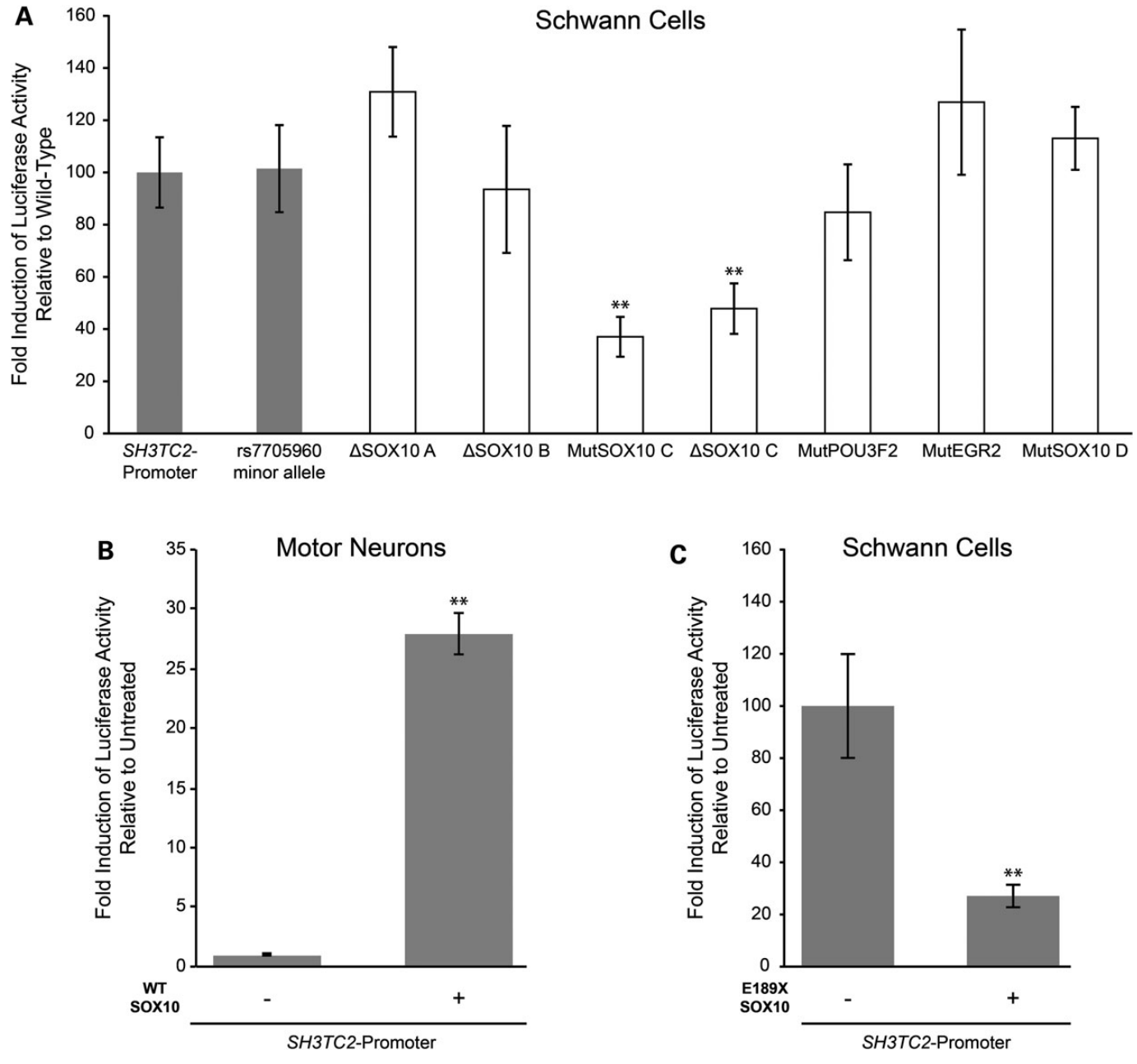

Figure 3. SOX10 regulates the *SH3TC2* promoter. (**A**) Constructs harboring the wild-type *SH3TC2* promoter, the promoter with the minor allele of rs7705960 or the promoter with the indicated mutation (all upstream of a luciferase reporter gene) were transfected into cultured Schwann (S16) cells. Luciferase assays were performed to determine the regulatory activity of each promoter segment relative to the wild-type *SH3TC2* promoter. Gray columns indicate naturally occurring sequences, whereas white columns indicate synthetic mutations. 'Mut' denotes mutation of the consensus sequence by reversing but not complementing the nucleotides, and 'Δ' denotes a complete deletion of the consensus sequence (see text for details). (**B**) A construct harboring the *SH3TC2* promoter directing luciferase expression was transfected into cultured motor neurons (MN-1 cells) with or without a construct to express wild-type (WT) SOX10. Luciferase assays were employed to test the activity of the *SH3TC2* promoter in the presence of SOX10 relative to the activity of the promoter in the absence of SOX10. (**C**) A construct harboring the *SH3TC2* promoter directing luciferase expression was transfected into cultured Schwann (S16) cells with or without a construct to express a dominant-negative form of SOX10 (E189X). Luciferase assays were employed to test the activity of the *SH3TC2* promoter in the presence of E189X SOX10 relative to the activity of the promoter in the absence of E189X SOX10. In each panel, error bars indicate standard deviations and ** indicates a significant change in activity ($P \leq 0.001$).

Fig. S2). These data suggest that the alleles of SNPs rs12519780, rs114059937 and rs17539452 modify the enhancer activity of *SH3TC2*-MCS5.

To identify the SNP(s) responsible for the decrease in *SH3TC2*-MCS5 Hap 4 activity, we mutagenized *SH3TC2*-MCS5 to harbor the minor allele of rs12519780, rs114059937 or rs17539452 alone or in various combinations (Mut A–E, Fig. 4B). Subsequently, each construct was tested for the ability to direct luciferase reporter gene expression in S16 cells relative to Hap 1. Expression constructs containing the minor

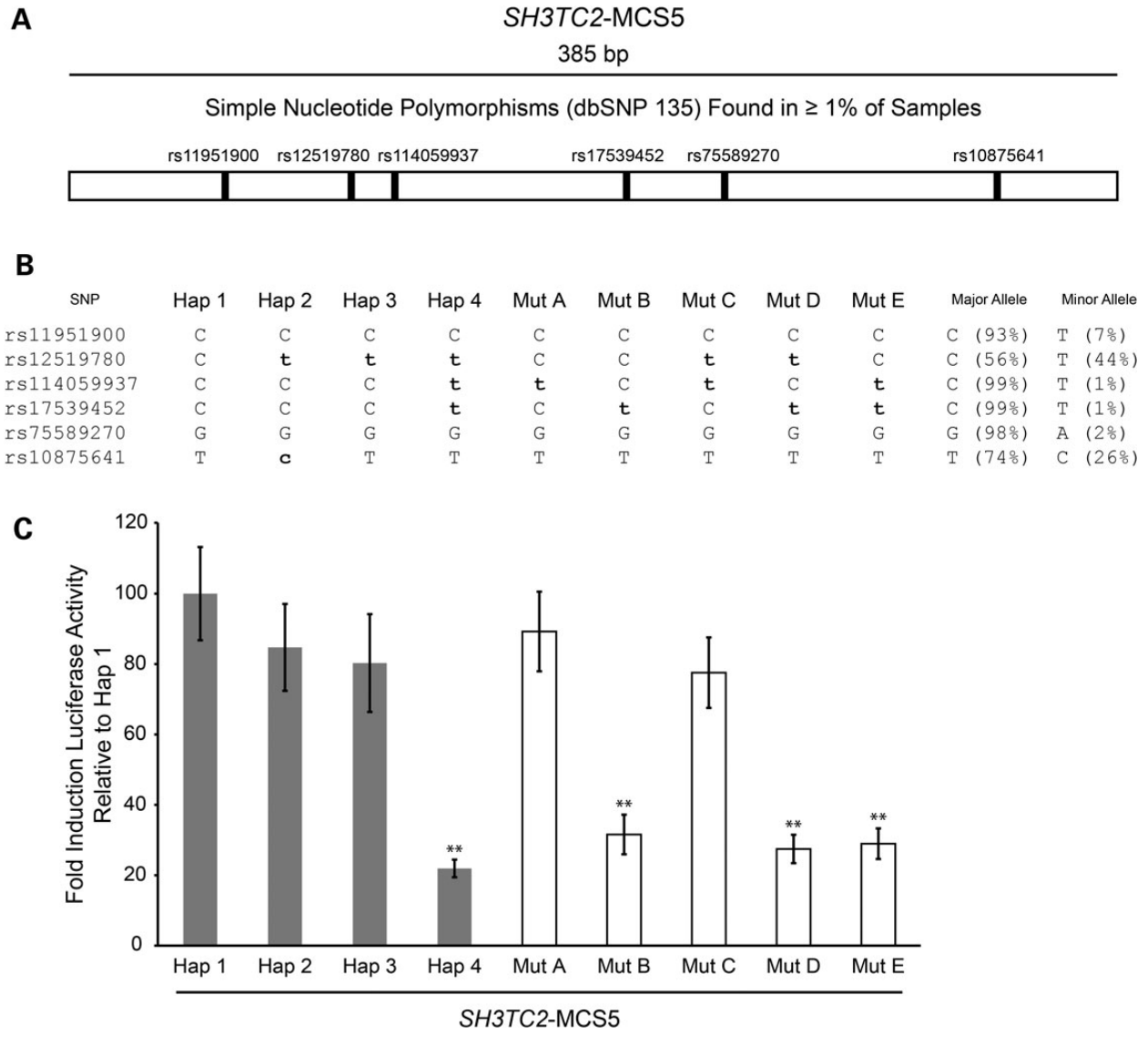

Figure 4. Haplotype-specific regulatory activity of *SH3TC2*-MCS5. (**A**) The *SH3TC2*-MCS5 amplicon (black line) spans 385 bp. The six SNPs with a minor allele frequency ≥0.01 that map within this region are indicated by vertical black lines. (**B**) *SH3TC2*-MCS5 was cloned from a pooled sample of human genomic DNA allowing the acquisition of four naturally occurring haplotypes (Hap 1–4). Synthetic haplotypes (Mut A–E) were engineered via mutagenesis. Each haplotype is indicated across the top and each SNP accession number indicated on the left. Major alleles are capitalized and minor alleles are in bold, lower-case text. Major and minor allele frequencies are listed on the right. (**C**) Each of the nine haplotypes at *SH3TC2*-MCS5 was cloned upstream of a luciferase reporter gene and transfected into cultured Schwann (S16) cells. Luciferase assays were performed to determine the regulatory activity of each genomic segment relative to Hap 1. Naturally occurring and synthetic haplotypes are indicated by gray and white bars, respectively. Error bars represent standard deviations and **indicates a significant change in activity ($P \leq 0.001$).

alleles of rs12519780 or rs114059937 alone (Hap 3 and Mut A, respectively) or combined together (Mut C) did not exhibit significantly reduced activities compared with Hap 1. In contrast, constructs harboring the minor allele of rs17539452 alone (Mut B, *P*-value 1.77×10^{-6}) or combined with the minor allele of rs12519780 (Mut D, *P*-value 1.87×10^{-9}) or rs114059937 (Mut E, *P*-value 1.46×10^{-9}) all showed at least a 70% reduction in enhancer activity in cultured Schwann cells compared with Hap 1 (Fig. 4C). These data indicate that the minor allele ('t' nucleotide) of rs17539452 is responsible for the majority of the ∼80% decrease in enhancer activity of *SH3TC2*-MCS5 Hap 4.

The minor allele of rs17539452 disrupts a cAMP response element binding protein (CREB) in *SH3TC2*-MCS5

One possible explanation for the reduced activity of *SH3TC2*-MCS5 Hap 4 (Fig. 4C) is that the minor allele of rs17539452 interferes with transcription factor binding. To test this, we analyzed 24 bp surrounding each allele of rs17539452 using the TRANSFAC transcription factor prediction algorithm (25). This revealed a cAMP response element (CRE) prediction for the major allele of rs17539452 that is not predicted for the minor allele (Fig. 5A and B; Supplementary Material, Fig. S3A and B). CREs are genomic elements that regulate

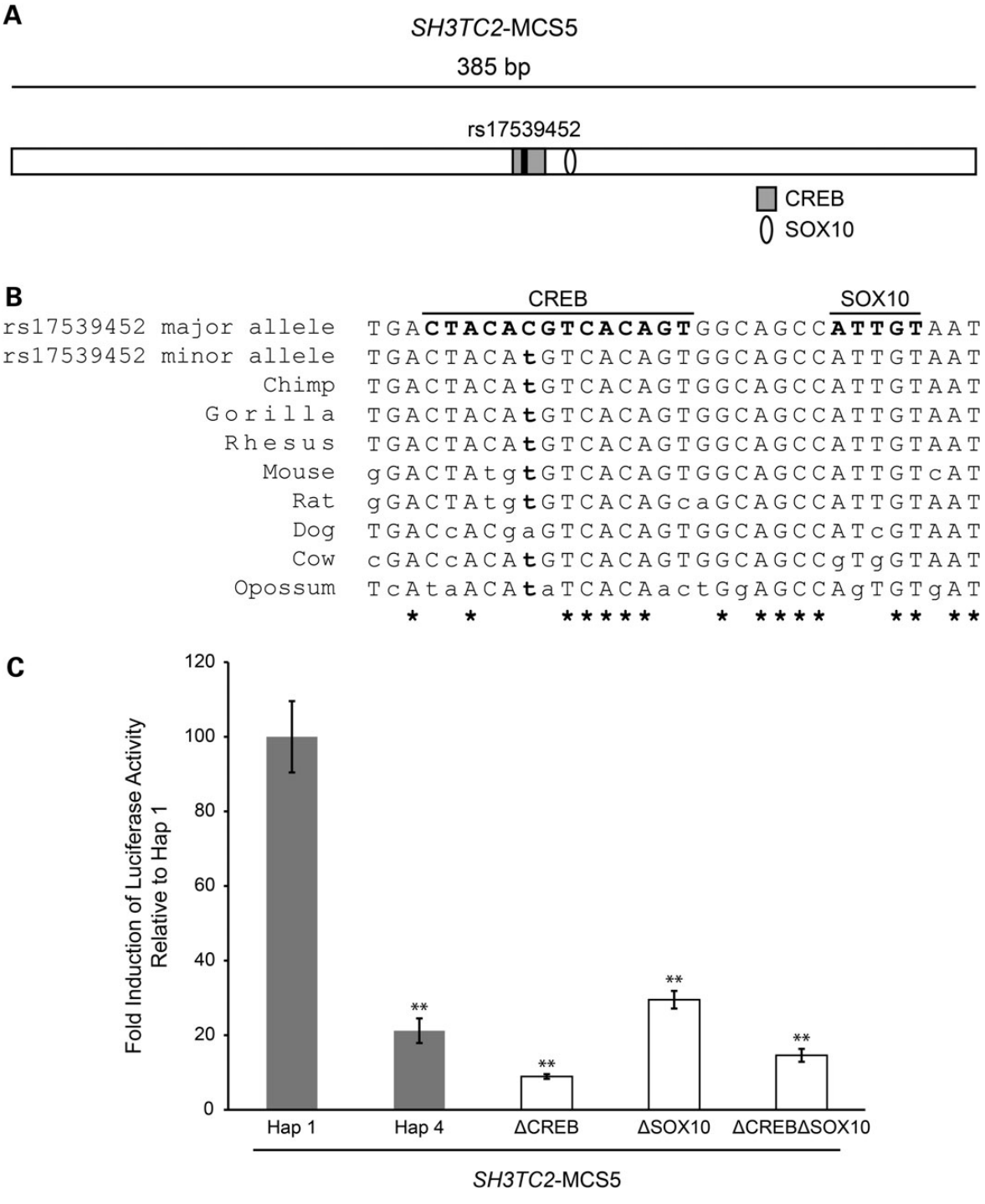

Figure 5. The minor allele of rs17539452 disrupts a CREB consensus sequence. (**A**) A cartoon depicting *SH3TC2*-MCS5. The CREB and SOX10 consensus sequences are indicated with a gray box and white oval, respectively. SNP rs17539452 is indicated within the CREB consensus sequence with a vertical black line. (**B**) Orthologous genomic sequences surrounding the CREB and SOX10 predictions from human (major and minor alleles of rs17539452) and eight additional mammalian species were aligned. CREB and SOX10 consensus sequences are indicated by capitalized, bold text. The minor allele of rs17539452 is in lower case, bold text. Lower case text indicates nucleotides that are not identical to the human major allele sequence and asterisks denote base pairs that are conserved across all of the shown species. (**C**) CREB and SOX10 consensus sequences were deleted (Δ), individually or together and the resulting *SH3TC2*-MCS5 genomic segments were cloned upstream of a luciferase reporter gene. Luciferase assays were performed to determine the regulatory activity of each genomic segment relative to Hap 1. Naturally occurring and synthetic alleles are indicated by gray and white bars, respectively. Error bars represent standard deviations and **indicates a significant change in activity ($P \leq 0.001$).

gene transcription in response to elevated cAMP. Intracellular cAMP induces phosphorylation of the CRE-binding (CREB) protein, predominantly via the PKA pathway, which can then bind to the CRE sequence and mediate transcriptional regulation (31). CREB is a ubiquitous transcription factor expressed in S16 cells (Supplementary Material, Fig. S3C); however, tissue-restricted CREB activity has been observed in melanocytes in cooperation with SOX10 (32). We therefore computationally analyzed *SH3TC2*-MCS5 for SOX10 consensus sequences as described above. These efforts revealed a single SOX10 monomeric consensus sequence 7 bp from the CREB consensus sequence (Fig. 5B and B). To assess the role of the CREB and SOX10 consensus sequences on the function of *SH3TC2*-MCS5, we generated luciferase reporter constructs harboring a deletion of the CREB consensus sequence (ΔCREB), a deletion of SOX10 consensus sequence (ΔSOX10), or a deletion of both consensus sequences (ΔCREBΔSOX10). Subsequently, each construct was transfected into S16 cells and enhancer activities were compared with *SH3TC2*-MCS5 Hap 1. All three deletions resulted in at least a 70% reduction in luciferase activity (*P*-values 2.25×10^{-8}, 4.68×10^{-8} and 1.91×10^{-8}, respectively; Fig. 5C). Importantly, the amount of activity associated with each deletion construct is comparable to that associated with Hap 4, which harbors the rs17539452 minor allele (Fig. 5C). These data indicate that the CREB and SOX10 consensus sequences are important for the observed enhancer activity of *SH3TC2*-MCS5.

SOX10 and CREB activate *SH3TC2*-MCS5 in Schwann cells

Our computational and functional data suggest that *SH3TC2*-MCS5 is responsive to the transcription factors SOX10 and CREB. To test this, we co-transfected the construct harboring *SH3TC2*-MCS5 Hap 1 upstream of a luciferase reporter gene with constructs to express wild-type SOX10 or CREB into SOX10-negative motor neurons (MN-1 cells) and SOX10-positive Schwann cells (S16 cells). In MN-1 cells, SOX10 and CREB both induced a >10-fold increase in activity compared with the untreated *SH3TC2*-MCS5 construct (*P*-values 1.92×10^{-7} and $1.83 \times {}^{-10}$, respectively; Fig. 6A); however, an additive effect was not observed (data not shown). In S16 cells, *SH3TC2*-MCS5 Hap 1 enhancer activity increased by 62% (*P*-value 0.00013) and 130% (*P*-value $1.34 \times {}^{-6}$) in the presence of additional SOX10 or CREB, respectively (Fig. 6B). Furthermore, an additive effect was observed when SOX10 and CREB were overexpressed together resulting in a 310% increase (*P*-value 9.06×10^{-13}) in activity (Fig. 6B). These data indicate that SOX10 and CREB activate *SH3TC2*-MCS5 in a synergistic fashion in Schwann cells.

To determine if endogenous SOX10 and CREB activate *SH3TC2*-MCS5 in S16 Schwann cells, we performed luciferase assays in the presence of a dominant-negative (E189X) SOX10 expression construct (30) or ascorbic acid (33) to inhibit the activity of endogenous SOX10 and CREB, respectively. Expression of dominant-negative SOX10 reduced the enhancer activity of *SH3TC2*-MCS5 Hap 1 by ∼65% (*P*-value $4.25 \times {}^{-10}$; Fig. 6C) and application of ascorbic acid reduced the activity of *SH3TC2*-MCS5 Hap 1 by ∼21% (*P*-value = 0.00078; Fig. 6D). To verify the effect of ascorbic acid on cultured S16 cells, we measured cAMP levels in untreated cells and those treated with 600 or 1000 μM ascorbic acid. This revealed a dose-dependent decrease in cAMP levels (Supplementary Material, Fig. S4A) consistent with the effect of ascorbic acid on the activity of *SH3TC2*-MCS5. Furthermore, to determine the specificity of ascorbic acid and dominant-negative SOX10 on *SH3TC2*-MCS5 activity, we performed luciferase assays on S16 cells transfected with the ΔCREBΔSOX10 *SH3TC2*-MCS5 luciferase expression construct in the presence of ascorbic acid or E189X SOX10. Neither of these conditions reduced luciferase activity (Supplementary Material, Fig. S4B and C), indicating that the effect of each requires the respective transcription factor binding site. Collectively, these data are consistent with SOX10 and CREB regulating the activity of *SH3TC2*-MCS5.

CREB binds to *SH3TC2*-MCS5

The reduced activity of *SH3TC2*-MCS5 Hap 4 may be due to decreased binding of the rs17539452 minor allele to nuclear proteins in Schwann cells. To test this, we utilized electromobility shift assays (EMSAs). Briefly, a biotinylated-DNA probe containing the CREB and SOX10 consensus sequences and the major allele of rs17539452 ('Maj' in Fig. 7A) was incubated with nuclear protein isolated from S16 Schwann cells. In the absence of nuclear protein, unbound DNA probe migrates to the bottom of the gel (lane 1, Fig. 7A). When S16 cell nuclear protein is present, a distinct pattern of shifted bands is observed indicating that the probe binds to nuclear protein from Schwann cells (lane 2, Fig. 7A). Competition with increasing amounts of a cold 'Maj' competitor probe (lanes 3 and 4, Fig. 7A) caused a decrease in signal for one specific protein-bound DNA band (arrowhead, Fig. 7A). We infer that this band corresponds to a specific interaction between the 'Maj' biotin probe and S16 nuclear proteins. Competition with a probe designed around the minor allele of rs17539452 ('Min' in Fig. 7A) does not outcompete the binding as effectively as the 'Maj' competitor probe at 100× (compare lanes 4 and 5, Fig. 7A), consistent with the minor allele of rs17539452 having reduced binding to Schwann cell nuclear proteins.

To determine if the 'Maj' biotin-labeled probe binds specifically to CREB, we performed a 'supershift' EMSA using an anti-CREB antibody. The addition of increasing amounts of antibody resulted in a corresponding decrease in signal intensity of the same band outcompeted by the 'Maj' competitor probe in standard EMSAs (arrowhead in Fig. 7B, compare lane 2 to lanes 3 through 5). This suggests that CREB binds to the 'Maj' biotin probe and that the presence of the CREB antibody prevents this interaction, possibly by disrupting the DNA binding capabilities of CREB. These results are similar to previously published 'supershift' EMSA data using the same antibody employed here (34). Furthermore, CREB binding profiles generated by ChIP-Seq (35) show significant binding of CREB at *SH3TC2*-MCS5 in multiple human cell lines (Supplementary Material, Fig. S1B). Combined, these data indicate that CREB binds to the region surrounding rs17539452 and that the minor allele of this SNP impairs CREB.

Forskolin increases the expression of *Sh3tc2* in Schwann cells *in vivo*

Our data thus far raise the possibility that *SH3TC2* is a CREB target gene. To test this, we utilized forskolin, a well-characterized adenylyl cyclase activator that increases the levels of cAMP and

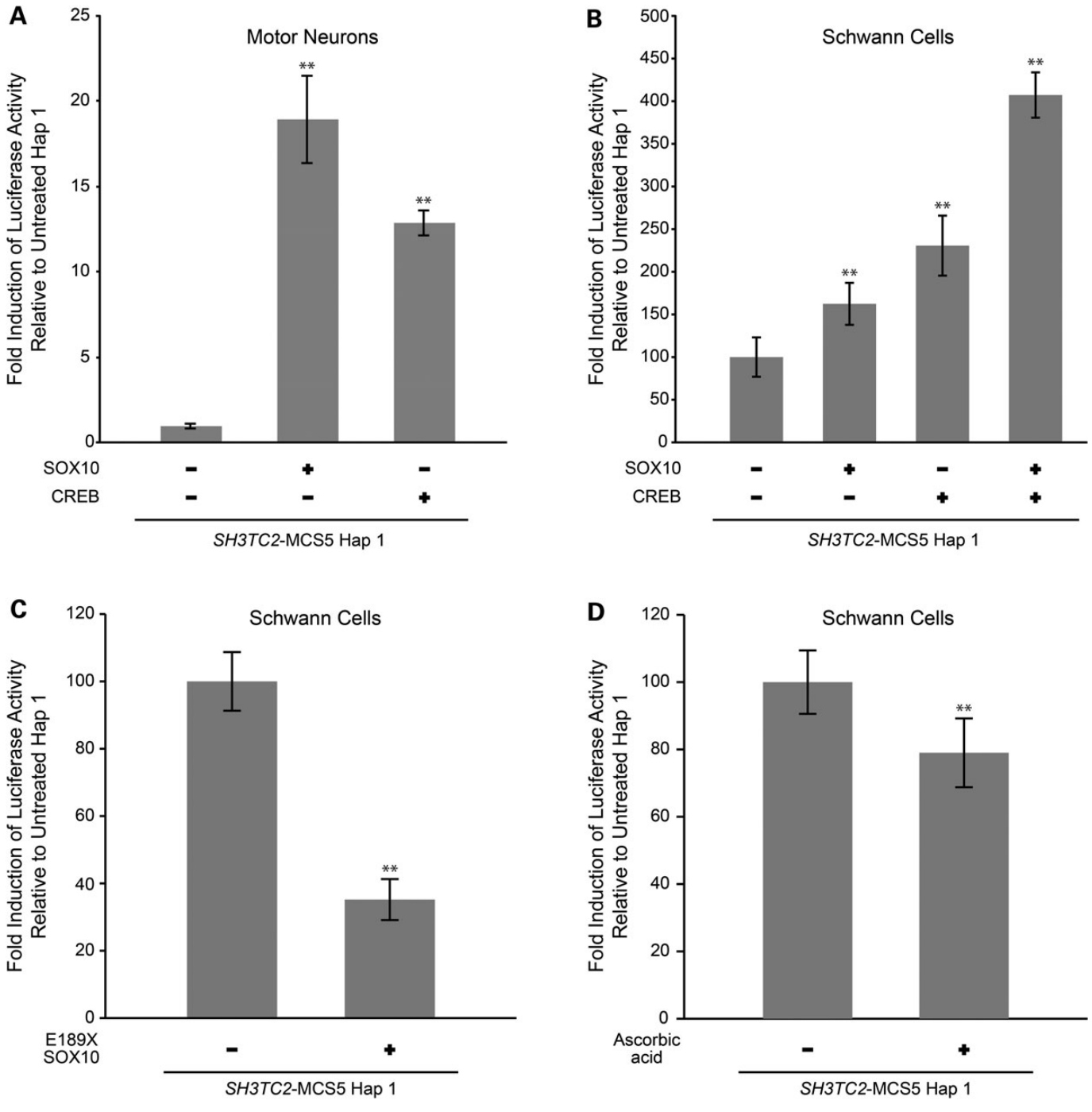

Figure 6. SOX10 and CREB activate *SH3TC2*-MCS5. (**A**) Constructs harboring *SH3TC2*-MCS5 Hap 1 were transfected into SOX10-negative motor neurons (MN-1 cells) with or without constructs to express SOX10 or CREB. Luciferase assays were performed to determine the effect of each transcription factor on the activity of *SH3TC2*-MCS5 relative to experiments without SOX10 and CREB. (**B**) Similar experiments as described in (A) performed in cultured Schwann (S16) cells. Note that in this experiment SOX10 and CREB have an additive effect on the activity of *SH3TC2*-MCS5. (**C** and **D**) Luciferase assays were also performed to determine the effect of dominant-negative (E189X) SOX10 (C) and ascorbic acid (D) on *SH3TC2*-MCS5 activity. In all panels, error bars indicate standard deviations and ** indicates a significant change in activity ($P \leq 0.001$).

activates CREB via the PKA pathway (36). Briefly, rat primary Schwann cells were treated with 3 μM forskolin for 24 h after which RNA was extracted and mRNA expression measured by quantitative RT-PCR. Treatment with forskolin induced a significant increase in the expression of *Sh3tc2*, *Pmp22* and *Egr2* (Fig. 7C); the latter gene encodes a master transcription factor of myelination. Importantly, the induction of *Sh3tc2* is comparable to that of *Pmp22*, which harbors a characterized CREB response element in the promoter (37). Another Schwann cell gene, *Sox10*, whose expression is unaffected by altered cAMP

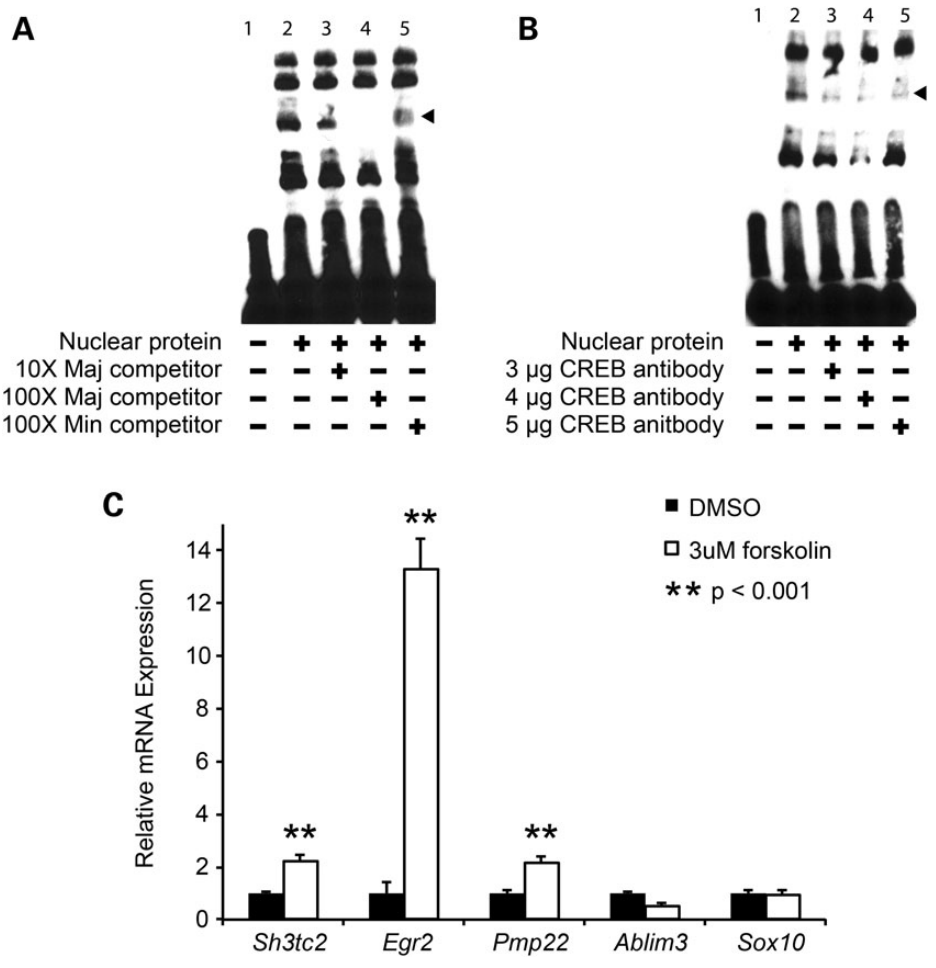

Figure 7. The cAMP/CREB pathway interacts with the *SH3TC2* locus. (**A**) EMSAs were performed on nuclear extracts from cultured Schwann (S16) cells using a biotinylated probe carrying the major allele (Maj) of SNP rs17539452. Competition between labeled and unlabeled Maj probes, and between labeled Maj and unlabeled Min probes (the latter harboring the minor allele of SNP rs17539452) were performed to determine the specificity of DNA binding. The nuclear protein and competitor probe content of each lane is indicated across the bottom. Reactions in all lanes contain the same amount of labeled Maj probe. (**B**) 'Supershift' EMSAs were performed on nuclear extracts from cultured Schwann (S16) cells in the presence of increasing amounts of CREB antibody (indicated along the bottom). Arrowheads in (A) and (B) indicate specific interactions between nuclear proteins and labeled probe. (**C**) Rat primary Schwann cells were serum starved overnight and then treated with forskolin (3 μM) or DMSO (control) for 24 h. Quantitative RT-PCR was then performed on RNA isolated from each sample to determine the expression level of each endogenous gene (indicated along the bottom). All data were normalized to the level of 18S rRNA and expressed relative to the DMSO-only control sample. Double asterisks (**) indicate a change in gene expression ($P \leq 0.001$) and error bars represent standard error.

production (38,39) is shown as a control. We also examined the effect of forskolin on the two loci flanking *Sh3tc2*: *Ablim3* and *Adrb2*. These studies revealed that *Ablim3* is not induced by forskolin (Fig. 7C) and that *Adrb2* is not expressed in rat primary Schwann cells (data not shown). Combined, these data are consistent with CREB directly activating *Sh3tc2* expression in Schwann cells via *SH3TC2*-MCS5.

Common SNPs at the *SH3TC2* locus are associated with CMT disease severity

The identification of a regulatory SNP at *SH3TC2* suggests that this variant (or other functional variants at *SH3TC2*) may modify CMT disease phenotypes. We studied a cohort of 407 exceptionally phenotyped patients with CMT1A that were collected under strict clinical protocols by the Inherited Neuropathy Consortium (INC). CMT1A is caused by a duplication event of a canonical area of chromosome 17 containing the *PMP22* gene (17–19). On the background of this uniform mutation, we sought to identify genotypes at *SH3TC2* that are associated with variable expression of key clinical outcomes in patients with CMT1A. Genome-wide SNP genotyping was utilized to test the hypothesis that common variation at the *SH3TC2* locus (Supplementary Material, Fig. S4), particularly in the region surrounding rs17539452, is associated with CMT1A disease expression. Association was tested using the CAPL software (40). Nominal association was found with a 'difficulty walking' subphenotype (rs2082383, *P*-value = 0.048, 33 kb proximal to rs17539452; and rs6580586, *P*-value = 0.0194, 50 kb proximal), a 'decrease in feeling' subphenotype (rs1029942, *P*-value = 0.0141, 17 kb distal; and rs2082383, *P*-value = 0.00857, 33 kb proximal) and a 'foot dorsiflexion' subphenotype (rs4555784, *P*-value = 0.0479, 50 kb distal). There was no association with 'difficulty with balance' among the SNPs within 50 kb of rs17539452.

In addition to the region surrounding rs17539452, we examined SNPs within and adjacent to the *SH3TC2* transcriptional unit (Supplementary Material, Fig. S4) for association with CMT1A disease severity. Three SNPs were associated with 'foot dorsiflexion' and 'decrease in feeling': (i) a nonsynonymous change (rs6875902, p.Ala468Ser; *P*-value = 0.0068), (ii) a 3′-UTR change (rs3763022; *P*-value = 0.0025) and (iii) an intronic change (rs2304034; *P*-value = 0.037). The nonsynonymous change is moderately conserved with a GERP score of 0.802. Thus, our genetic analyses have revealed an association between genotypes at *SH3TC2* and phenotypic outcome in CMT1A disease. However, due to the low minor allele frequency of rs17539452 (0.021 in individuals of European descent from the HapMap dataset), reliable association tests and linkage disequilibrium patterns could not be generated in our moderately sized patient cohort.

DISCUSSION

In this study, we describe transcriptional regulatory elements at the *SH3TC2* locus, which is implicated in autosomal recessive CMT disease type 4C (CMT4C). Our analyses identified a promoter and downstream enhancer that are active in Schwann cells *in vitro*. The promoter region is regulated by the neural crest/Schwann cell transcription factor SOX10 based on multiple lines of evidence. Overexpression of wild-type SOX10 causes increased induction in promoter activity in SOX10-negative cells, and overexpression of dominant-negative SOX10, which prevents endogenous SOX10 from binding to DNA (30), causes decreased promoter activity in cultured Schwann cells. SOX10 regulation of the *SH3TC2* promoter likely occurs via a head-to-head SOX10 binding site located 96 bp upstream of the TSS, because mutating this site causes a dramatic reduction in promoter activity. Recent ChIP-Seq analysis of transcription factor binding sites in rat Schwann cells (28) revealed a single SOX10 binding peak at the *SH3TC2* promoter near the head-to-head SOX10 site described here. Since no other SOX10 consensus sequence within the promoter significantly contributes to regulatory activity, we conclude that our analyses have revealed the specific sequences required for SOX10 induction of the *SH3TC2* promoter.

We also characterized a distal enhancer at *SH3TC2* ~150 kb downstream of the TSS. Based on similar experiments performed at the *SH3TC2* promoter, we conclude that the downstream enhancer is regulated by the transcription factors SOX10 and CREB. Interestingly, while we present strong evidence of CREB binding at *SH3TC2*-MCS5, significant levels of SOX10 binding were not detected at this region in ChIP-Seq analyses performed on rat sciatic nerves (28). One possible explanation for this discrepancy is that this enhancer may be active at an earlier developmental stage than that assessed in the ChIP-Seq studies (see below). Indeed, based on the effect of deleting the SOX10 binding site and the specificity of overexpressing wild-type and dominant-negative SOX10, we are confident that *SH3TC2*-MCS5 is a CREB/SOX10 response element. One of the difficulties of analyzing *cis*-acting transcriptional regulatory elements is determining the specific gene(s) that they regulate. This is especially problematic when a regulatory element maps to an intergenic region, as is the case with the downstream enhancer described here. However, we showed that SOX10 and CREB synergistically activate the downstream enhancer and that forskolin treatment, which activates CREB, induces *Sh3tc2* mRNA transcription *in vivo*. In contrast, *Adrb2* (the next locus downstream of *Sh3tc2*) is not expressed in Schwann cells and *Ablim3* (the next locus upstream of *Sh3tc2*) is not induced by forskolin. Finally, the induction of *Sh3tc2* expression by forskolin is comparable to that of *Pmp22*, which is a known CREB target gene in Schwann cells (37). Collectively, these data support the conclusion that *SH3TC2* is regulated by SOX10 and CREB via the downstream enhancer.

SOX10 and cAMP have important roles in Schwann cell development and peripheral nervous system (PNS) myelination. SOX10 is expressed early in neural crest development and remains active in myelinating Schwann cells throughout development and adulthood (41–43). SOX10 interacts with other transcription factors important for regulating Schwann cell myelination including EGR2, POU3F2 and POU3F1/SCIP/OCT6 (26,44). While consensus sequences for EGR2 and POU3F2 were found within the *SH3TC2* promoter (Fig. 2), these were not necessary for regulatory activity (Fig. 3). Furthermore, ChIP-Seq and expression studies have shown that SOX10 regulates *Sh3tc2* independent of EGR2 (28). Intracellular cAMP plays an essential role in transitioning immature Schwann cells to myelinating Schwann cells by activating CREB (38,39,45,46). As mentioned above, co-expression of SOX10 and CREB revealed a synergistic effect on the activity of the downstream enhancer (*SH3TC2*-MCS5). Synergism between CREB and SOX10 was previously observed at the *MITF* locus in melanocytes (32), and other myelin genes are regulated by SOX10 and CREB including *PMP22* (37,47,48), *EGR2* (49–51) and *OCT6* (38,52). While synergism between SOX10 and CREB has not been demonstrated at these latter three loci, it is clear that co-regulation by SOX10 and CREB is an important aspect of Schwann cell myelination.

Transcriptional regulation of *SH3TC2* by cAMP/CREB may provide insight into how an increase in intracellular cAMP induces Schwann cell myelination (45). It was recently demonstrated that SH3TC2 interacts with the receptor ERBB2 in Schwann cells, resulting in internalization of ERBB2 from the adaxonal membrane (11). The Nrg1/ERBB signaling pathway is important for the regulation of Schwann cell proliferation and migration as well as for Schwann cell differentiation and myelination (10). The mechanism by which Nrg1/ERBB signaling switches between the two pathways is unclear; however, increasing intracellular cAMP causes the Nrg1/ERBB signaling cascade to direct Schwann cells to differentiate and myelinate the associated axon (45). Furthermore, impaired cAMP production results in the absence of myelinated peripheral nerve axons in *Gpr126* mutant mice and zebrafish (38,39), and *Sh3tc2*-null mice exhibit hypomyelinated peripheral nerves (6). Combined, these data suggest that decreased cAMP production and impaired SH3TC2 function may disrupt a common pathway in PNS myelination. Our data indicate that cAMP/CREB induces *SH3TC2* transcription. Therefore, we hypothesize that increased cAMP levels induce myelination by enhancing *SH3TC2* transcription (likely via the downstream enhancer) and increasing ERBB2 internalization.

Characterization of the *SH3TC2* promoter and downstream enhancer will facilitate the identification of pathogenic regulatory mutations that confer disease by disrupting *SH3TC2*

transcription. CMT4C is an autosomal recessive disease caused by loss-of-function mutations (7–9). Mutations disrupting a regulatory element may cause a loss-of-function effect by reducing or ablating *SH3TC2* transcription. Indeed, while regulatory mutations have not been identified at *SH3TC2*, they may account for the missing heritability observed in patients with a CMT4C phenotype that are heterozygous for only one *SH3TC2* coding mutation (15,16); however, our analysis of six such patients revealed no variants in the promoter or *SH3TC2*-MCS5 (data not shown). Additionally, the rs17539452 minor allele might directly cause disease in patients with CMT4C that are compound heterozygous for the minor allele and a second mutation—the predicted reduction in *SH3TC2* expression caused by the minor allele, in combination with a second mutant allele at *SH3TC2*, may be enough to cause disease symptoms. Thus, we strongly recommend: (i) the inclusion of the regulatory elements described here in future mutation screens of patients with a recessive demyelinating CMT disease phenotype and (ii) evaluation of rs17539452 in CMT disease onset in patients with unexplained CMT4C disease.

An important, yet unexplored area of CMT disease research is the identification of genetic modifiers to explain the high clinical variability observed among patients with CMT disease, especially among those carrying the same genetic lesion (53). Determining the transcriptional regulation of CMT-associated genes will facilitate the identification of genetic modifiers that reside in regulatory elements and alter the expression of key PNS genes. We hypothesized that the SNP rs17539452 is an excellent candidate modifier of CMT disease since the presence of the minor allele in the downstream *SH3TC2* enhancer perturbs CREB binding and reduces enhancer activity. CMT1A is the most common form of CMT disease and is caused by duplication of ~1.5 Mb on chromosome 17, which harbors the *PMP22* gene (17–19). While nearly all patients with CMT1A carry an identical duplication (54), it has long been noted that phenotypic expression varies even within the same family. On the background of this common *PMP22* mutation, we tested if SNPs at *SH3TC2* are associated with specific phenotypic outcomes in the largest cohort of uniformly phenotyped patients with CMT1A collected to date. Indeed, while our genetic studies did not have the power to detect an effect of the non-coding regulatory SNP described here (rs17539452), we did observe a number of significant correlations ($P < 0.05$) between SNP genotypes and CMT1A disease severity. These data are hypothesis driven due to the known importance of *SH3TC2* in PNS myelination, however replication in an additional patient cohort will be required to validate these findings. Additionally, it will be important to demonstrate a correlation between the genotype of the SNPs studied here and *SH3TC2* expression or protein function; however, the former studies are complicated by the Schwann cell-specific expression of this gene.

Finally, the data presented here may have implications for designing strategies to treat patients with CMT1A disease. Increased expression of *PMP22* is the pathogenic mechanism of CMT1A disease, and it has been proposed that decreasing *PMP22* expression will alleviate the clinical phenotype. Upon finding that CREB positively regulates the *PMP22* promoter (37), it was posited that treatment with ascorbic acid, which reduces CREB function, may reduce *PMP22* expression and benefit patients with CMT1A. Indeed, mice with a *PMP22*-overexpression-induced neuropathy showed dramatic behavioral and histopathological improvement upon treatment with ascorbic acid (55). However, initial clinical trials on young and adult patients with CMT1A have not revealed any benefits of ascorbic acid treatment (56–59). One reason for the lack of improvement in patients may be due to a deleterious effect of ascorbic acid on CREB response loci such as *EGR2*, *OCT6* and *SH3TC2*, as well as other, undiscovered CREB target loci. Furthermore, the success of ascorbic acid treatment in mouse may reflect differential effects on gene expression between rodents and human. Interestingly, the CREB-responsive major allele of the SNP we characterized in the downstream enhancer (*SH3TC2*-MCS5) is human specific. These data also raise the possibility that certain human loci have developed a special requirement for CREB function in Schwann cells. Addressing this will require defining the full panel of CREB target genes in Schwann cells and assessing for differences in gene expression and regulatory activity between human and rodents.

In summary, we have characterized transcriptional regulatory elements at *SH3TC2* that are activated by the transcription factors SOX10 and CREB. These findings revealed: (i) additional regions for mutation screening in patients with CMT4C, (ii) a SNP allele that dramatically reduces the activity of a downstream enhancer, (iii) a novel target gene of CREB in Schwann cells and (iv) specific SNPs at *SH3TC2* that are associated with phenotypic differences in patients with CMT1A. As research on the genetics and genomics of CMT disease moves further toward whole-genome interrogation, efforts should focus on a broader assessment of regulatory SNPs in peripheral nerve function and CMT disease etiology, which will likely reveal pathways to exploit for therapeutic development.

MATERIALS AND METHODS

Comparative sequence analysis at the *SH3TC2* locus

The following sequences from orthologous *SH3TC2* loci were obtained from the UCSC Genome Browser (60): human (chr5: 148 188 390–148 501 247, hg18), mouse (chr18:62 047 106–62 352 470, mm9), rat (chr18:57 898 589–58 181 925, rn4), dog (chr4:62 992 595–63 262 602, canFam2), cow (chr7:62 226 792–62 510 218, bosTau6) and opossum (chr1:377 577 553–377 972 236, monDom5). Repetitive DNA sequences were masked using the UCSC Genome Browser 'Sequence Formatting Options' and each genomic sequence was submitted to the MultiPipMaker alignment algorithm (21). The human genomic sequence at *SH3TC2* was used as the reference, and the 'Search both strands' and 'Chaining' options were employed. Subsequently, the MultiPipMaker 'acgt' alignment file was submitted to the EP algorithm (http://research.nhgri.nih.gov/exactplus/) (22) using the following settings: minimum length of exact match to seed = 5, minimum number of species to seed = 6 and minimum number of species to extend an alignment = 6.

Transcription factor binding site predictions

To identify Schwann-cell relevant transcription factor binding sites in the *SH3TC2* promoter and *SH3TC2*-MCS5, we submitted each genomic sequence (Table 1) to the TRANSFAC

transcription factor prediction program using the MATCH algorithm (25), the 'minimize the sum of both error rates' setting, and the following matrices: V$BRN2_01, V$EGR2_01, V$POU3F2_01, V$POU3F2_02, V$SOX10_Q6 and an in-house SOX10 consensus sequence 'ACAMD' (where 'M' is a C or A nucleotide and 'D' is a G, T or A nucleotide). To identify transcription factor consensus sequences that are differentially predicted on the major and minor alleles of rs17539452, we submitted 24 bp of genomic sequence surrounding each allele [GGATGACTACAcGTCACAGTGGCA (major allele) and GGATGACTACAtGTCACAGTGGCA (minor allele)] to the TRANSFAC transcription factor prediction program using the MATCH algorithm (25), the 'minimize the sum of both error rates' setting and the 'vertebrate, non-redundant' matrix database.

Expression vector construction

Oligonucleotide primers containing attB1 and attB2 Gateway cloning sequences (Invitrogen) were designed for PCR-based amplification of the *SH3TC2* promoter and each *SH3TC2*-MCS region (Supplementary Material, Table S1). Subsequent to PCR amplification and purification, each genomic segment was cloned into the pDONR221 vector using BP Clonase (Invitrogen). Resulting constructs were genotyped by digestion with *Bsr*GI (New England Biolabs) and subjected to DNA sequence analysis to ensure sequence specificity. Each resulting pDONR221 construct was recombined with a destination vector harboring a minimal promoter directing a luciferase reporter gene (pE1B-luciferase) (22) using LR Clonase (Invitrogen). Successful cloning of each genomic segment upstream of the luciferase reporter gene was assessed by genotyping with *Bsr*GI (New England Biolabs).

Site-directed mutagenesis reactions were performed using the QuikChange II Mutagenesis Kit (Agilent Technologies) and appropriate mutation-bearing primers (Supplementary Material, Table S1). Mutagenesis primers were designed to delete or mutate specific transcription factor consensus sequences or to introduce specific alleles of SNPs. Mutagenesis was performed in pDONR221 constructs (see above), and each resulting clone was subjected to DNA sequence analysis to ensure that only the desired mutation was introduced into the insert. Correctly mutagenized inserts were recombined into the luciferase reporter gene construct as described above.

Cell culture and luciferase assays

Immortalized rat Schwann cells (S16) (61) and mouse spinal motor neurons (MN-1) (62) were grown in Dulbecco's modified Eagle's medium supplemented with 10% fetal bovine serum and 2 mM L-glutamine. Cells were incubated at 37°C in 5% CO_2. 1×10^4 cells were plated in a 96-well culture plate (Corning Life Sciences) and incubated overnight. Subsequently, cells were transfected with luciferase expression constructs using Lipofectamine 2000 (Invitrogen) according to the manufacturer's specifications. Each well was transfected with 200 ng of the indicated luciferase expression construct and 2 ng of a renilla expression construct (to control for transfection efficiency and cell viability) in 50 μl of Opti-MEM and 0.25 μl Lipofectamine (Invitrogen) cocktail as previously described (63). For overexpression of each transcription factor, 100 ng of wild-type SOX10, dominant-negative E189X SOX10 (30) or wild-type CREB (Clontech) expression constructs were co-transfected into each reaction. Cells were incubated in the transfection solution for 4 h and then cultured in normal growth media. For ascorbic acid treatment, growth media was supplemented with 600 μM ascorbic acid (Sigma–Aldrich) and the effect on cAMP levels was evaluated using the cAMP-Glo™ Max Assay (Promega) according to the manufacturer's specifications. After 48 h, cells were lysed in 20 μl of passive lysis buffer (Promega) for 1 h and 10 μl of each lysate was transferred to a polystyrene 96-well assay plate (Corning Life Sciences). Luciferase and renilla activities were then determined using the Dual Luciferase Reporter Assay System (Promega) and a Glomax Multi-Detection System (Promega). Each experiment was performed at least 24 times using at least two different DNA preparations per construct. The ratio of luciferase to renilla activity and the fold increase in the ratio relative to a control luciferase expression vector with no insert ('Empty' in figures) were calculated. The mean (bar height in figures) and standard deviation (error bars in figures) were determined using standard calculations. Statistical significance was performed using a two-tailed Student's *t*-test where * and ** indicate a *P*-value <0.01 and 0.001, respectively.

5′ Rapid amplification of cDNA ends

First-strand cDNA was generated from RNA isolated from rat cultured Schwann (S16) cells using an oligonucleotide primer designed within exon 4 of the rat *Sh3tc2* gene (5′-tttcctccagg gtcttgaagg-3′). The cDNA sample was subsequently TdT-tailed using the 5′ RACE System (Invitrogen) and sequential PCR reactions were performed using nested primers (Supplementary Material, Table S1). PCR products were separated on 1% low-melt agarose gels, excised and purified using the QIAquick Gel Extraction Kit (Qiagen), and subjected to DNA sequence analysis.

Electromobility shift assay

S16 nuclear extracts were prepared using the NE-PER Nuclear and Cytoplasmic Protein Extraction Kit (Thermo Fisher Scientific). 5′-biotin-labeled and unlabeled complimentary oligonucleotides (Supplementary Material, Table S1) were annealed to form biotinylated and competitor probes, respectively. EMSAs were performed using the LightShift Chemiluminescent EMSA Kit (Thermo Fisher Scientific) according to the manufacturer's specifications. Briefly, 5 μg of S16 nuclear extract was incubated with or without an unlabeled competitor probe (10× and 100×) in a 20 μl binding reaction containing 1× binding buffer and 50 ng Poly(dI.dC) for 20 min at room temperature. Subsequently, 20 fmol of biotinylated probe was added to each binding reaction and incubated for an additional 20 min at room temperature. Binding reactions were electrophoresed on a 6% TBE DNA retardation gel (Invitrogen) and transferred to a positively charged nylon membrane (Roche) using a semi-dry transfer unit (Bio-Rad). DNA was crosslinked to the membrane using the Spectrolinker 2000 (Spectronics). Chemiluminescent detection of the biotinylated probes was performed with a streptavidin-horseradish peroxidase conjugate (Thermo Fisher Scientific) and exposed to X-ray film. For

'supershift' EMSAs, varying amounts (0, 3, 4 and 5 μg) of CREB antibody (C-21; Santa Cruz Biotechnology) were incubated with S16 nuclear extract prior to adding the labeled probe.

Western blot analyses

Cultured S16, MN-1 and HeLa cells were harvested and resuspended in 37.5 μl of lysis solution containing 10 mM Tris–HCl/1 mM EDTA/50 mM NaCl (Invitrogen) and 12.5 μl of loading buffer containing SDS (Invitrogen). After incubation at 95°C for 5 min, the protein lysate was electrophoresed on 4–12% Bis–Tris gels (Invitrogen) at 125 V for 100 min in running buffer containing SDS (Invitrogen). Samples were then electroblotted onto nitrocellulose membranes at 25 V for 100 min in NuPAGE transfer buffer (Invitrogen). Membranes were blocked in 1× PBS/0.05% Tween 20/5% non-fat dry milk for 18 h at 4°C and then incubated with a 1:1000 dilution of anti-CREB antibody (C-21; Santa Cruz Biotechnology) in blocking solution for 1 h at room temperature. Membranes were washed three times in 1× PBS plus 0.05% Tween 20, incubated with a secondary antibody conjugated to horseradish peroxidase for 1 h at room temperature, washed three times as described above and incubated with DAB substrate (Roche Diagnostics), according to the manufacturer's instructions.

Sh3tc2 expression studies

Rat primary Schwann cells were cultured as previously described (64). Cells were treated with 3 μM forskolin (Sigma–Aldrich) in DMSO or an equivalent volume of only DMSO (control) for 24 h after which total mRNA was extracted using Trizol (Invitrogen). One microgram of total RNA from each sample was used to prepare cDNA as previously described (65). Quantitative RT–PCR was performed by monitoring in real time the increase in fluorescence of the SYBR-GREEN dye as described (66) using the TaqMan 7000 Sequence Detection System (Applied Biosystems). Relative amounts of each transcript between samples were determined using the comparative C_t method (67) and normalized to levels of 18S rRNA. Primer sequences are listed in Supplementary Material, Table S1.

Genotyping DNA samples from patients with CMT1A

Four hundred and seven patients with the classic CMT1A-causing *PMP22* duplication were ascertained under a protocol developed by the INC. IRB approval was obtained from all participating sites and all patients were consented accordingly. Detailed phenotypic assessment was performed by board-certified neurologists and, for this study, four categories of outcome were defined that capture the major features of peripheral neuropathies: 'difficulty walking', 'decrease in feeling', 'difficulty in balance' and 'foot dorsiflexion'. Genotyping was performed using the Illumina Human OmniExpress 12v1; however, only SNPs in the vicinity of *SH3TC2* were extracted for this study (Supplementary Material, Fig. S4). Association was tested using the Combined Association in the Presence of Linkage (CAPL) software (40). CAPL performs statistical association tests, allowing for the inclusion of family data and population substructure.

SUPPLEMENTARY MATERIAL

Supplementary Material is available at *HMG* online.

ACKNOWLEDGEMENTS

The authors thank Chani Hodonsky for excellent technical assistance; Richard Quarles for the S16 cell line; Kurt Fischbeck for the MN-1 cell line; Jim Lupski, Ken Inoue and Michael Wegner for SOX10 expression constructs; the laboratory of Miriam Meisler for thoughtful discussions; Pavel Seeman and Kurt Fischbeck for DNA samples from patients with CMT4C; and the members of the Inherited Neuropathy Consortium for contributing DNA samples from phenotyped patients with CMT1A, which were essential for the association studies presented here.

Conflict of Interest statement. None declared.

FUNDING

This work was funded by grants from the National Institute of Neurological Diseases and Stroke to A.A. (NS073748) and J.S. (NS075269) and the Rare Disease Clinical Research Center for Inherited Neuropathies (U54NS065712). M.H.B. was a recipient of the Sir Keith Murdoch Fellowship from the American Australian Association, and F.B. was supported by the Princess Beatrix Spier Fund (PBF; grant WAR08-18).

REFERENCES

1. Skre, H. (1974) Genetic and clinical aspects of Charcot-Marie-Tooth's disease. *Clin. Genet.*, **6**, 98–118.
2. Senderek, J., Bergmann, C., Stendel, C., Kirfel, J., Verpoorten, N., De Jonghe, P., Timmerman, V., Chrast, R., Verheijen, M.H.G., Lemke, G. *et al.* (2003) Mutations in a gene encoding a novel SH3/TPR domain protein cause autosomal recessive Charcot-Marie-Tooth type 4C neuropathy. *Am. J. Hum. Genet.*, **73**, 1106–1119.
3. Azzedine, H., Ravisé, N., Verny, C., Gabrëels-Festen, A., Lammens, M., Grid, D., Vallat, J.M., Durosier, G., Senderek, J., Nouioua, S. *et al.* (2006) Spine deformities in Charcot-Marie-Tooth 4C caused by SH3TC2 gene mutations. *Neurology*, **67**, 602–606.
4. Yger, M., Stojkovic, T., Tardieu, S., Maisonobe, T., Brice, A., Echaniz-Laguna, A., Alembik, Y., Girard, S., Cazeneuve, C., Leguern, E. *et al.* (2012) Characteristics of clinical and electrophysiological pattern of Charcot-Marie-Tooth 4C. *J. Peripher. Nerv. Syst.*, **17**, 112–122.
5. Lupski, J.R., Reid, J.G., Gonzaga-Jauregui, C., Rio Deiros, D., Chen, D.C.Y., Nazareth, L., Bainbridge, M., Dinh, H., Jing, C., Wheeler, D.A. *et al.* (2010) Whole-genome sequencing in a patient with Charcot-Marie-Tooth neuropathy. *N. Engl. J. Med.*, **362**, 1181–1191.
6. Arnaud, E., Zenker, J., de Preux Charles, A.S., Stendel, C., Roos, A., Medard, J.J., Tricaud, N., Kleine, H., Luscher, B., Weis, J. *et al.* (2009) SH3TC2/KIAA1985 protein is required for proper myelination and the integrity of the node of Ranvier in the peripheral nervous system. *Proc. Natl. Acad. Sci. USA*, **106**, 17528–17533.
7. Lupo, V., Galindo, M.I., Martínez-Rubio, D., Sevilla, T., Vílchez, J.J., Palau, F. and Espinós, C. (2009) Missense mutations in the SH3TC2 protein causing Charcot-Marie-Tooth disease type 4C affect its localization in the plasma membrane and endocytic pathway. *Hum. Mol. Genet.*, **18**, 4603–4614.
8. Stendel, C., Roos, A., Kleine, H., Arnaud, E., Ozçelik, M., Sidiropoulos, P.N.M., Zenker, J., Schüpfer, F., Lehmann, U., Sobota, R.M. *et al.* (2010) SH3TC2, a protein mutant in Charcot-Marie-Tooth neuropathy, links peripheral nerve myelination to endosomal recycling. *Brain*, **133**, 2462–2474.
9. Roberts, R.C., Peden, A.A., Buss, F., Bright, N.A., Latouche, M., Reilly, M.M., Kendrick-Jones, J. and Luzio, J.P. (2010) Mistargeting of SH3TC2

away from the recycling endosome causes Charcot-Marie-Tooth disease type 4C. *Hum. Mol. Genet.*, **19**, 1009–1018.
10. Newbern, J. and Birchmeier, C. (2010) Nrg1/ErbB signaling networks in Schwann cell development and myelination. *Semin. Cell Dev. Biol.*, **21**, 922–928.
11. Gouttenoire, E.A., Lupo, V., Calpena, E., Bartesaghi, L., Schüpfer, F., Médard, J.-J., Maurer, F., Beckmann, J.S., Senderek, J., Palau, F. *et al.* (2013) Sh3tc2 deficiency affects neuregulin-1/ErbB signaling. *Glia*, **61**, 1041–1051.
12. Gooding, R., Colomer, J., King, R., Angelicheva, D., Marns, L., Parman, Y., Chandler, D., Bertranpetit, J. and Kalaydjieva, L. (2005) A novel Gypsy founder mutation, p.Arg1109X in the CMT4C gene, causes variable peripheral neuropathy phenotypes. *J. Med. Genet.*, **42**, e69.
13. Colomer, J., Gooding, R., Angelicheva, D., King, R.H.M., Guillén-Navarro, E., Parman, Y., Nascimento, A., Conill, J. and Kalaydjieva, L. (2006) Clinical spectrum of CMT4C disease in patients homozygous for the p.Arg1109X mutation in SH3TC2. *Neuromuscular Disord.*, **16**, 449–453.
14. Laššuthová, P., Gregor, M., Sarnová, L., Machalová, E., Sedláček, R. and Seeman, P. (2012) Clinical, in silico, and experimental evidence for pathogenicity of two novel splice site mutations in the SH3TC2 gene. *J. Neurogenet.*, **26**, 413–420.
15. Laššuthová, P., Mazanec, R., Vondráček, P., Sišková, D., Haberlova, J., Sabová, J. and Seeman, P. (2011) High frequency of SH3TC2 mutations in Czech HMSN I patients. *Clin. Genet.*, **80**, 334–345.
16. Gosselin, I., Thiffault, I., Tétreault, M., Chau, V., Dicaire, M.-J., Loisel, L., Emond, M., Senderek, J., Mathieu, J., Dupré, N. *et al.* (2008) Founder SH3TC2 mutations are responsible for a CMT4C French-Canadians cluster. *Neuromuscular Disord.*, **18**, 483–492.
17. Lupski, J.R., de Oca-Luna, R.M., Slaugenhaupt, S., Pentao, L., Guzzetta, V., Trask, B.J., Saucedo-Cardenas, O., Barker, D.F., Killian, J.M., Garcia, C.A. *et al.* (1991) DNA duplication associated with Charcot-Marie-Tooth disease type 1A. *Cell*, **66**, 219–232.
18. Timmerman, V., Nelis, E., Van Hul, W., Nieuwenhuijsen, B.W., Chen, K.L., Wang, S., Ben Othman, K., Cullen, B., Leach, R.J. and Hanemann, C.O. (1992) The peripheral myelin protein gene PMP-22 is contained within the Charcot-Marie-Tooth disease type 1A duplication. *Nat. Genet.*, **1**, 171–175.
19. Patel, P.I., Roa, B.B., Welcher, A.A., Schoener-Scott, R., Trask, B.J., Pentao, L., Snipes, G.J., Garcia, C.A., Francke, U., Shooter, E.M. *et al.* (1992) The gene for the peripheral myelin protein PMP-22 is a candidate for Charcot-Marie-Tooth disease type 1A. *Nat. Genet.*, **1**, 159–165.
20. Antonellis, A. and Green, E.D. (2008) Inter-species comparative sequence analysis: a tool for genomic medicine. In Willard, H. and Ginsburg, G. (eds), *Genomic and Personalized Medicine*. Academic Press, Salt Lake City, pp. 120–130.
21. Elnitski, L., Burhans, R., Riemer, C., Hardison, R. and Miller, W. (2010) MultiPipMaker: a comparative alignment server for multiple DNA sequences. *Curr. Protoc. Bioinformatics*, **10**, Unit10.4.
22. Antonellis, A., Bennett, W.R., Menheniott, T.R., Prasad, A.B. and Lee-Lin, S.-Q., NISC Comparative Sequencing Program, Green, E.D., Paisley, D., Kelsh, R.N., Pavan, W.J. *et al.* (2006) Deletion of long-range sequences at Sox10 compromises developmental expression in a mouse model of Waardenburg-Shah (WS4) syndrome. *Hum. Mol. Genet.*, **15**, 259–271.
23. Hai, M., Muja, N., DeVries, G.H., Quarles, R.H. and Patel, P.I. (2002) Comparative analysis of Schwann cell lines as model systems for myelin gene transcription studies. *J. Neurosci. Res.*, **69**, 497–508.
24. Hodonsky, C.J., Kleinbrink, E.L., Charney, K.N., Prasad, M., Bessling, S.L., Jones, E.A., Srinivasan, R., Svaren, J., McCallion, A.S. and Antonellis, A. (2011) SOX10 regulates expression of the SH3-domain kinase binding protein 1 (Sh3kbp1) locus in Schwann cells via an alternative promoter. *Mol. Cell. Neurosci.*, **49**, 85–96.
25. Matys, V., Kel-Margoulis, O.V., Fricke, E., Liebich, I., Land, S., Barre-Dirrie, A., Reuter, I., Chekmenev, D., Krull, M., Hornischer, K. *et al.* (2006) TRANSFAC and its module TRANSCompel: transcriptional gene regulation in eukaryotes. *Nucleic Acids Res.*, **34**, D108–D110.
26. Svaren, J. and Meijer, D. (2008) The molecular machinery of myelin gene transcription in Schwann cells. *Glia*, **56**, 1541–1551.
27. Peirano, R.I. and Wegner, M. (2000) The glial transcription factor Sox10 binds to DNA both as monomer and dimer with different functional consequences. *Nucleic Acids Res.*, **28**, 3047–3055.
28. Srinivasan, R., Sun, G., Keles, S., Jones, E.A., Jang, S.W., Krueger, C., Moran, J.J. and Svaren, J. (2012) Genome-wide analysis of EGR2/SOX10 binding in myelinating peripheral nerve. *Nucleic Acids Res.*, **40**, 6449–6460.
29. Lee, K.E., Nam, S., Cho, E.-A., Seong, I., Limb, J.-K., Lee, S. and Kim, J. (2008) Identification of direct regulatory targets of the transcription factor Sox10 based on function and conservation. *BMC Genomics*, **9**, 408.
30. Inoue, K., Khajavi, M., Ohyama, T., Hirabayashi, S.-I., Wilson, J., Reggin, J.D., Mancias, P., Butler, I.J., Wilkinson, M.F., Wegner, M. *et al.* (2004) Molecular mechanism for distinct neurological phenotypes conveyed by allelic truncating mutations. *Nat. Genet.*, **36**, 361–369.
31. Lee, K.A. and Masson, N. (1993) Transcriptional regulation by CREB and its relatives. *Biochim. Biophys. Acta*, **1174**, 221–233.
32. Huber, W.E., Price, E.R., Widlund, H.R., Du, J., Davis, I.J., Wegner, M. and Fisher, D.E. (2003) A tissue-restricted cAMP transcriptional response: SOX10 modulates alpha-melanocyte-stimulating hormone-triggered expression of microphthalmia-associated transcription factor in melanocytes. *J. Biol. Chem.*, **278**, 45224–45230.
33. Kaya, F., Belin, S., Diamantidis, G. and Fontés, M. (2008) Ascorbic acid is a regulator of the intracellular cAMP concentration: old molecule, new functions? *FEBS Lett.*, **582**, 3614–3618.
34. Xue, H., Qiao, Y., Ni, P., Wang, J., Chen, C. and Huang, G. (2011) A CRE that binds CREB and contributes to PKA-dependent regulation of the proximal promoter of human RAB25 gene. *Int. J. Biochem. Cell Biol.*, **43**, 348–357.
35. ENCODE Project ConsortiumDunham, I., Kundaje, A., Aldred, S.F., Collins, P.J., Davis, C.A., Doyle, F., Epstein, C.B., Frietze, S., Harrow, J. *et al.* (2012) An integrated encyclopedia of DNA elements in the human genome. *Nature*, **489**, 57–74.
36. Insel, P.A. and Ostrom, R.S. (2003) Forskolin as a tool for examining adenylyl cyclase expression, regulation, and G protein signaling. *Cell. Mol. Neurobiol.*, **23**, 305–314.
37. Sabéran-Djoneidi, D., Sanguedolce, V., Assouline, Z., Lévy, N., Passage, E. and Fontés, M. (2000) Molecular dissection of the Schwann cell specific promoter of the PMP22 gene. *Gene*, **248**, 223–231.
38. Monk, K.R., Naylor, S.G., Glenn, T.D., Mercurio, S., Perlin, J.R., Dominguez, C., Moens, C.B. and Talbot, W.S. (2009) A G protein-coupled receptor is essential for Schwann cells to initiate myelination. *Science*, **325**, 1402–1405.
39. Monk, K.R., Oshima, K., Jörs, S., Heller, S. and Talbot, W.S. (2011) Gpr126 is essential for peripheral nerve development and myelination in mammals. *Development*, **138**, 2673–2680.
40. Chung, R.-H., Schmidt, M.A. and Martin, E.R. (2011) CAPL: an efficient association software package using family and case-control data and accounting for population stratification. *BMC Bioinformatics*, **12**, 201.
41. Kuhlbrodt, K., Herbarth, B., Sock, E., Hermans-Borgmeyer, I. and Wegner, M. (1998) Sox10, a novel transcriptional modulator in glial cells. *J. Neurosci.*, **18**, 237–250.
42. Britsch, S., Goerich, D.E., Riethmacher, D., Peirano, R.I., Rossner, M., Nave, K.A., Birchmeier, C. and Wegner, M. (2001) The transcription factor Sox10 is a key regulator of peripheral glial development. *Genes Dev.*, **15**, 66–78.
43. Bremer, M., Fröb, F., Kichko, T., Reeh, P., Tamm, E.R., Suter, U. and Wegner, M. (2011) Sox10 is required for Schwann-cell homeostasis and myelin maintenance in the adult peripheral nerve. *Glia*, **59**, 1022–1032.
44. Reiprich, S., Kriesch, J., Schreiner, S. and Wegner, M. (2010) Activation of Krox20 gene expression by Sox10 in myelinating Schwann cells. *J. Neurochem.*, **112**, 744–754.
45. Arthur-Farraj, P., Wanek, K., Hantke, J., Davis, C.M., Jayakar, A., Parkinson, D.B., Mirsky, R. and Jessen, K.R. (2011) Mouse schwann cells need both NRG1 and cyclic AMP to myelinate. *Glia*, **59**, 720–733.
46. Guo, L., Lee, A.A., Rizvi, T.A., Ratner, N. and Kirschner, L.S. (2013) The protein kinase A regulatory subunit R1A (Prkar1a) plays critical roles in peripheral nerve development. *J. Neurosci.*, **33**, 17967–17975.
47. Jones, E.A., Lopez-Anido, C., Srinivasan, R., Krueger, C., Chang, L.-W., Nagarajan, R. and Svaren, J. (2011) Regulation of the PMP22 Gene through an intronic enhancer. *J. Neurosci.*, **31**, 4242–4250.
48. Jones, E.A., Brewer, M.H., Srinivasan, R., Krueger, C., Sun, G., Charney, K.N., Keles, S., Antonellis, A. and Svaren, J. (2012) Distal enhancers upstream of the Charcot-Marie-Tooth type 1A disease gene PMP22. *Hum. Mol. Genet.*, **21**, 1581–1591.
49. Ghislain, J. and Charnay, P. (2006) Control of myelination in Schwann cells: a Krox20 cis-regulatory element integrates Oct6, Brn2 and Sox10 activities. *EMBO Rep.*, **7**, 52–58.
50. Chavrier, P., Janssen-Timmen, U., Mattéi, M.G., Zerial, M., Bravo, R. and Charnay, P. (1989) Structure, chromosome location, and expression of the

mouse zinc finger gene Krox-20: multiple gene products and coregulation with the proto-oncogene c-fos. *Mol. Cell. Biol.*, **9**, 787–797.
51. Alexandre, C., Charnay, P. and Verrier, B. (1991) Transactivation of Krox-20 and Krox-24 promoters by the HTLV-1 Tax protein through common regulatory elements. *Oncogene*, **6**, 1851–1857.
52. Jagalur, N.B., Ghazvini, M., Mandemakers, W., Driegen, S., Maas, A., Jones, E.A., Jaegle, M., Grosveld, F., Svaren, J. and Meijer, D. (2011) Functional dissection of the Oct6 Schwann cell enhancer reveals an essential role for dimeric Sox10 binding. *J. Neurosci.*, **31**, 8585–8594.
53. Thomas, P.K., Marques, W., Davis, M.B., Sweeney, M.G., King, R.H., Bradley, J.L., Muddle, J.R., Tyson, J., Malcolm, S. and Harding, A.E. (1997) The phenotypic manifestations of chromosome 17p11.2 duplication. *Brain*, **120**, 465–478.
54. Boerkoel, C.F., Takashima, H., Garcia, C.A., Olney, R.K., Johnson, J., Berry, K., Russo, P., Kennedy, S., Teebi, A.S., Scavina, M. *et al.* (2002) Charcot-Marie-Tooth disease and related neuropathies: mutation distribution and genotype-phenotype correlation. *Ann. Neurol.*, **51**, 190–201.
55. Passage, E., Norreel, J.C., Noack-Fraissignes, P., Sanguedolce, V., Pizant, J., Thirion, X., Robaglia-Schlupp, A., Pellissier, J.F. and Fontés, M. (2004) Ascorbic acid treatment corrects the phenotype of a mouse model of Charcot-Marie-Tooth disease. *Nat. Med.*, **10**, 396–401.
56. Micallef, J., Attarian, S., Dubourg, O., Gonnaud, P.-M., Hogrel, J.-Y., Stojkovic, T., Bernard, R., Jouve, E., Pitel, S., Vacherot, F. *et al.* (2009) Effect of ascorbic acid in patients with Charcot-Marie-Tooth disease type 1A: a multicentre, randomised, double-blind, placebo-controlled trial. *Lancet Neurol.*, **8**, 1103–1110.
57. Verhamme, C., de Haan, R.J., Vermeulen, M., Baas, F., de Visser, M. and van Schaik, I.N. (2009) Oral high dose ascorbic acid treatment for one year in young CMT1A patients: a randomised, double-blind, placebo-controlled phase II trial. *BMC Med.*, **7**, 70.
58. Pareyson, D., Reilly, M.M., Schenone, A., Fabrizi, G.M., Cavallaro, T., Santoro, L., Vita, G., Quattrone, A., Padua, L., Gemignani, F. *et al.* (2011) Ascorbic acid in Charcot-Marie-Tooth disease type 1A (CMT-TRIAAL and CMT-TRAUK): a double-blind randomised trial. *Lancet Neurol.*, **10**, 320–328.
59. Lewis, R.A., McDermott, M.P., Herrmann, D.N., Hoke, A., Clawson, L.L., Siskind, C., Feely, S.M.E., Miller, L.J., Barohn, R.J., Smith, P. *et al.* (2013) High-dosage ascorbic acid treatment in Charcot-Marie-Tooth disease type 1A: results of a randomized, double-masked, controlled trial. *JAMA Neurol.*, **70**, 981–987.
60. Karolchik, D., Hinrichs, A.S. and Kent, W.J. (2011) The UCSC Genome Browser. *Curr. Protoc. Hum. Genet.*, **18**, Unit18.6.
61. Toda, K., Small, J.A., Goda, S. and Quarles, R.H. (1994) Biochemical and cellular properties of three immortalized Schwann cell lines expressing different levels of the myelin-associated glycoprotein. *J. Neurochem.*, **63**, 1646–1657.
62. Salazar-Grueso, E.F., Kim, S. and Kim, H. (1991) Embryonic mouse spinal cord motor neuron hybrid cells. *Neuroreport*, **2**, 505–508.
63. Antonellis, A., Huynh, J.L., Lee-Lin, S.-Q., Vinton, R.M., Renaud, G., Loftus, S.K., Elliot, G., Wolfsberg, T.G., Green, E.D., McCallion, A.S. *et al.* (2008) Identification of neural crest and glial enhancers at the mouse Sox10 locus through transgenesis in zebrafish. *PLoS Genet.*, **4**, e1000174.
64. Leblanc, S.E., Srinivasan, R., Ferri, C., Mager, G.M., Gillian-Daniel, A.L., Wrabetz, L. and Svaren, J. (2005) Regulation of cholesterol/lipid biosynthetic genes by Egr2/Krox20 during peripheral nerve myelination. *J. Neurochem.*, **93**, 737–748.
65. Lee, S.L., Wang, Y. and Milbrandt, J. (1996) Unimpaired macrophage differentiation and activation in mice lacking the zinc finger transplantation factor NGFI-A (EGR1). *Mol. Cell. Biol.*, **16**, 4566–4572.
66. Morrison, T.B., Weis, J.J. and Wittwer, C.T. (1998) Quantification of low-copy transcripts by continuous SYBR Green I monitoring during amplification. *Biotechniques*, **24**, 954–958.
67. Livak, K.J. and Schmittgen, T.D. (2001) Analysis of relative gene expression data using real-time quantitative PCR and the 2(-Delta Delta C(T)) method. *Methods*, **25**, 402–408.